For promoter region of CD86-2 gene

forward primer CD86-pro-F2-*Xho*I

5'-GCCTCGAGTGGGAGTGAGACAGACGCTGCACAGAGCTT-3'

reverse primer CD86-pro-R2-*Hin*dIII

5'- GCAAGCTTAAGTAAAAGGAGCCTTGTCCGCTCCCCAGG-3

Figure S1. Expression of CD80 and CD86 in murine BMDCs with various stimuli

Murine BMDCs were stimulated with/without LPS (1 μg/mL) and/or IFNγ (100 ng/mL) for 24 hours, followed by analysis of CD80 or CD86 by flow cytometry. A, Solid line histogram represents cells with each Ab. Dotted line histogram represents negative control with 2.4G2 alone. "Unstim." refers to treatment without any agents. B, Graph was generated with the relative mean fluorescence intensity (MFI) values obtained after normalization with MFI of negative control.

Figure S2. Schematic drawing of primer sets used for 5'-RACE (thin arrow) and for detection of transcripts in Fig. S3 (thick arrow)

Figure S3. mRNA expression levels of CD80 and CD86 in BMDCs

mRNA was prepared from murine BMDCs treated with IFNγ (100 ng/mL) for 24 hours, and/or following stimulation by LPS (1 μg/mL) for 1 hour or without any treatment. Quantification of CD80 and CD86 mRNAs was performed by real-time PCR.

Figure S4. Cell surface expression of CD80 and CD86 understimulation by multi-cytokine cocktails. Lineage-negative cells were transfected with pMX-IRES/GFP series and transfectants were monitored as GFP-positive cells. Histogram represents cells transfected with retrovirus vector encoding PU.1 cDNA or mock vector. Cells

were incubated with infectious viruses for 3 days in the presence of IL-3, IL-6, SCF, TPO and EPO with GM-CSF, G-CSF, M-CSF, and Flt3L. At 3 days after infection, cells were stimulated with/without 1 μg/ml LPS and/or 100 ng/ml IFNγ for 24 hours, and were then stained with PE-labeled mAbs and transfectants are monitored as GFP-positive cells. Solid line histogram represents cells with each Ab. Dotted line histogram represents negative control with 2.4G2 alone. Representative results are shown.

Figure S5. CD80 and CD86 siRNA suppressed CD80 and CD86 expression, respectively, but did not suppress PU.1 expression. Murine BMDCs were transfected with 2 μg of CD80 siRNA, CD86 siRNA, negative control siRNA (N.CTRL) or distilled water (vehicle). A, After 48-hour culture, total RNA was extracted from each transfectant, and the amounts of PU.1, CD80, CD86 and β-actin mRNAs were analyzed by ABI7500. PU.1, CD80 and CD86 mRNA levels are represented as the ratios against those of negative controls. The results are expressed as means + SD for 3 PCRs performed in duplicate. B, After 48-hour culture, cells were harvested and subjected to analysis for CD80 or CD86 by flow cytometry. Solid line histogram represents cells with each Ab. Dotted line histogram represents negative control with 2.4G2 alone. Representative results of two independent experiments are shown. C, mRNA expression levels of PU.1, CD80, and CD86 in siRNA-injected ears. Vehicle and negative control (n = 2), PU.1 siRNA (n = 4), CD80 siRNA and CD86 siRNA (n = 3).

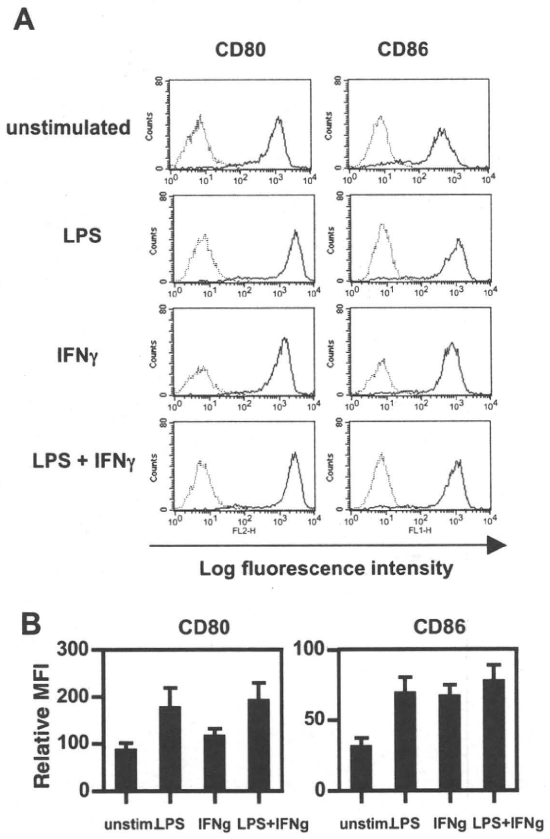
A
CD80
CD86
unstimulated
LPS
IFNγ
LPS + IFNγ
Counts
FL2-H
FL1-H
Log fluorescence intensity
B
CD80
CD86
Relative MFI
300
200
100
0
100
50
0
unstim
LPS
IFNg
LPS+IFNg

Figure S1

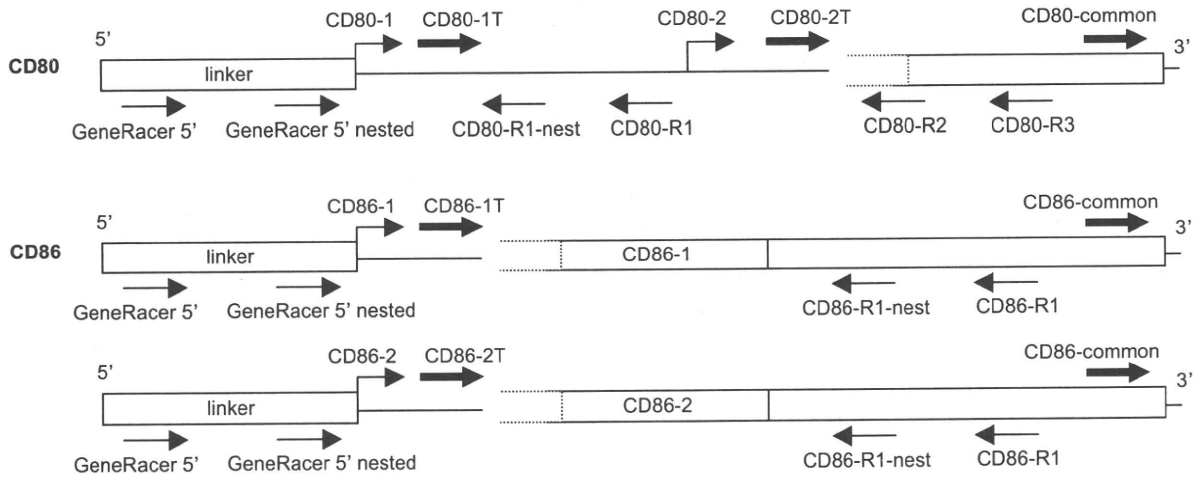
CD80
5'
linker
CD80-1
CD80-1T
CD80-2
CD80-2T
CD80-common
3'
GeneRacer 5'
GeneRacer 5' nested
CD80-R1-nest
CD80-R1
CD80-R2
CD80-R3
CD86
5'
linker
CD86-1
CD86-1T
CD86-common
3'
CD86-1
GeneRacer 5'
GeneRacer 5' nested
CD86-R1-nest
CD86-R1
5'
linker
CD86-2
CD86-2T
CD86-common
3'
CD86-2
GeneRacer 5'
GeneRacer 5' nested
CD86-R1-nest
CD86-R1

Figure S2

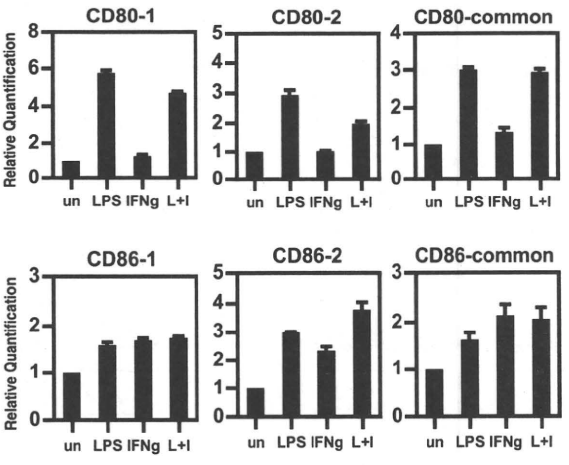
CD80-1
CD80-2
CD80-common
CD86-1
CD86-2
CD86-common
Relative Quantification
un
LPS
IFNg
L+I

Figure S3

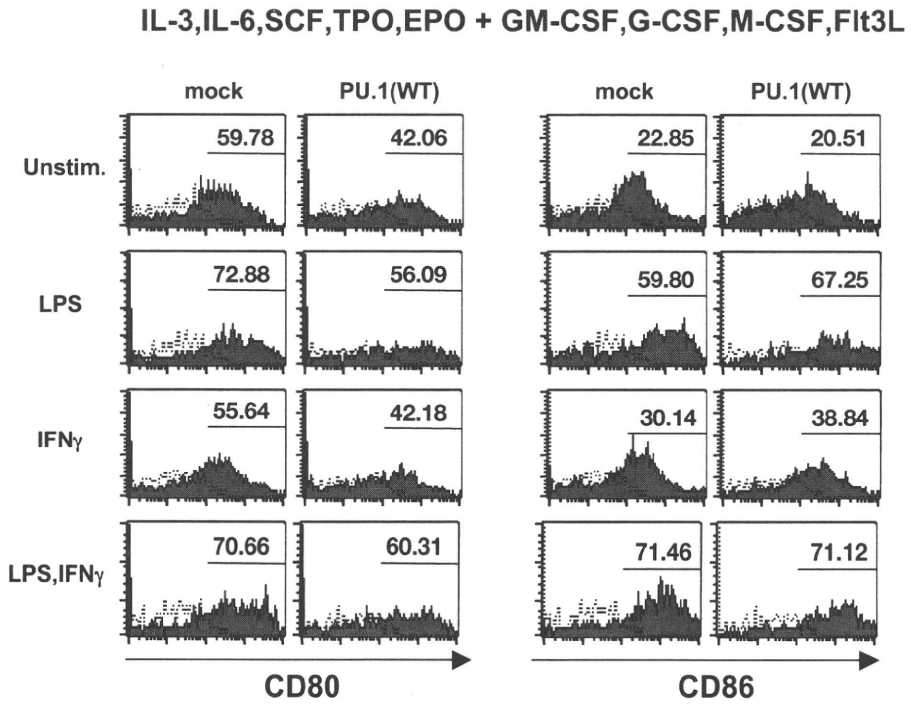
IL-3,IL-6,SCF,TPO,EPO + GM-CSF,G-CSF,M-CSF,Flt3L
mock
PU.1(WT)
mock
PU.1(WT)
Unstim.
59.78
42.06
22.85
20.51
LPS
72.88
56.09
59.80
67.25
IFNγ
55.64
42.18
30.14
38.84
LPS,IFNγ
70.66
60.31
71.46
71.12
CD80
CD86

Figure S4

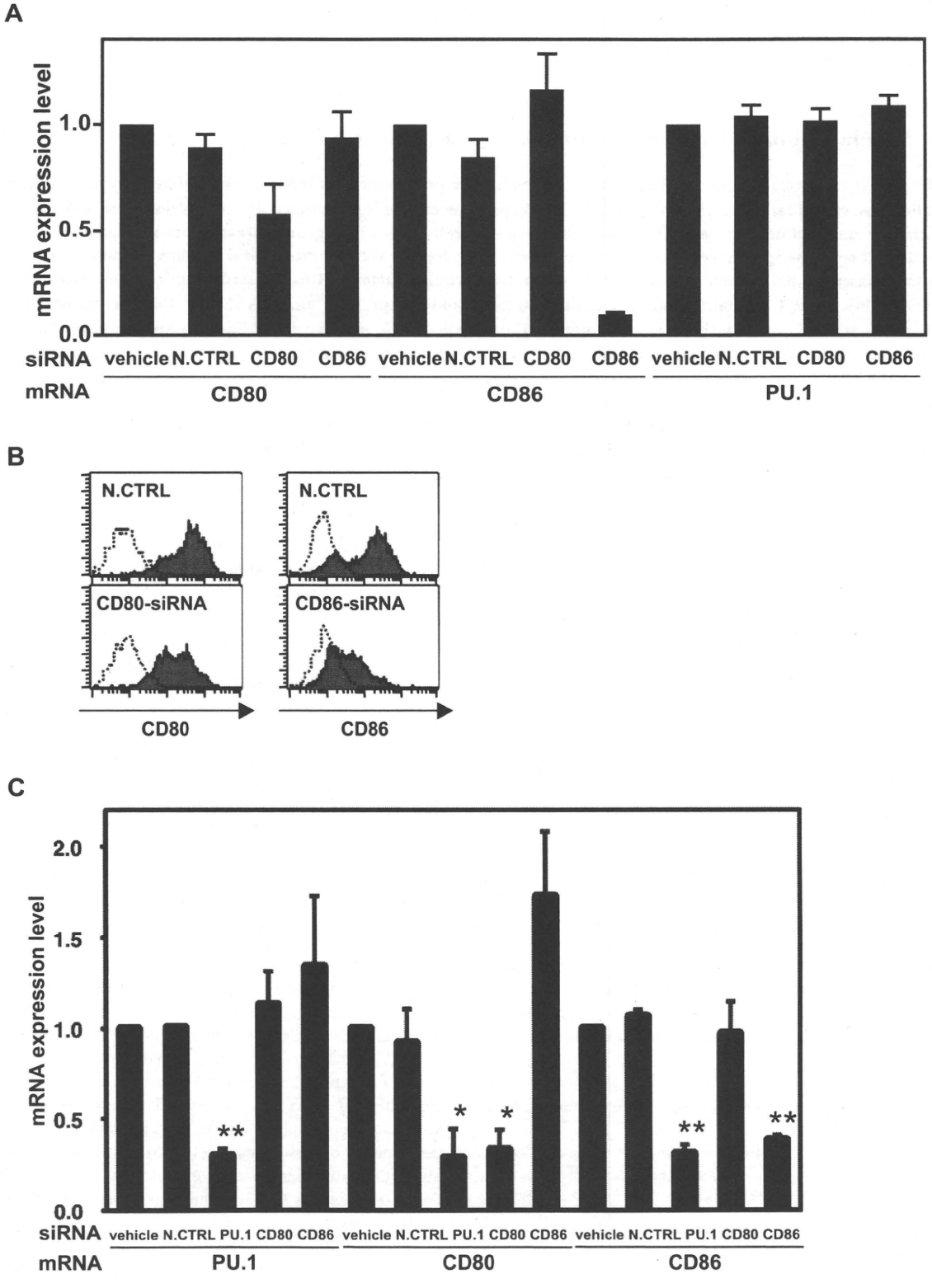
A
mRNA expression level
1.0
0.5
0.0
siRNA vehicle N.CTRL CD80 CD86 vehicle N.CTRL CD80 CD86 vehicle N.CTRL CD80 CD86
mRNA CD80 CD86 PU.1
B
N.CTRL
N.CTRL
CD80-siRNA
CD86-siRNA
CD80
CD86
C
mRNA expression level
2.0
1.5
1.0
0.5
0.0
**
*
*
**
**
siRNA vehicle N.CTRL PU.1 CD80 CD86 vehicle N.CTRL PU.1 CD80 CD86 vehicle N.CTRL PU.1 CD80 CD86
mRNA PU.1 CD80 CD86

Figure S5

GATA2 and Sp1 Positively Regulate the c-*kit* Promoter in Mast Cells

Keiko Maeda, Chiharu Nishiyama, Hideoki Ogawa, and Ko Okumura

The c-*kit* gene is expressed in hematopoietic stem cells and lineage progenitor cells but is downregulated during cell development in most lineages, except for mast cells. In mast cells, high expression of c-*kit* is maintained during development, and c-Kit signaling is essential for mast cell development. To analyze the mechanisms by which c-*kit* gene expression are regulated in mast cells, we examined mast cell type-specific regulation of the c-*kit* promoter region. We observed that a GC-box in the c-*kit* promoter was critical for transcriptional activity and was bound to the transcription factor Sp1 as assessed using reporter assay and electrophoretic mobility assay. Chromatin immunoprecipitation assay and coexpression analyses showed that the transcription factor GATA2, which was recruited to the c-*kit* promoter in a mast cell-specific manner, in addition to Sp1, transactivated the c-*kit* promoter via the GC-box. Electrophoretic mobility assay and rechromatin immunoprecipitation assay indicated that GATA2 binds to the GC-box by forming a complex with Sp1. Introduction of Sp1 small interfering RNA significantly reduced the amount not only of Sp1 but also of GATA2 binding to the c-*kit* promoter in mast cells, resulting in suppression of c-*kit* transcription. Knockdown of GATA2 suppressed the recruitment of GATA2 toward the c-*kit* promoter, subsequently suppressing cell surface expression of c-Kit. These findings indicate that GATA2 and Sp1 play crucial roles in expression of the c-*kit* gene in mast cells. *The Journal of Immunology*, 2010, 185: 4252–4260.

The c-*kit* gene encodes a receptor tyrosine kinase that is essential for hematopoiesis and is known as stem cell factor (SCF) receptor and is one of the specific markers of mast cells. In the hematopoietic system, c-*kit* is expressed in stem cells and linage progenitor cells, but is downregulated upon terminal erythrocyte and monocyte/macrophage development. In mast cells, c-*kit* is expressed throughout the developmental pathway to mature mast cells from hematopoietic stem cells, including mast cell progenitors (Lin^-, c-Kit^+, $Sca1^-$, $Ly6c^-$, $Fc\varepsilon RI\alpha^-$, CD27-$b7^+$, $T1/ST2^+$) in mouse adult bone marrow (1), and basophil and mast cell bipotent progenitors (Lin^-, c-Kit^+, $Fc\gamma RII/III^+$, $\beta7^+$) in mouse spleen (2). The c-Kit/SCF signaling is essential for mast cell development in both mice and humans as follows. *W* and *SI* mice, which have mutations in the chromosomal loci encoding c-Kit and SCF, respectively, have severely decreased numbers of mast cells (3, 4), and numerous *W* mutations affecting c-Kit structure and function have been identified and characterized. In the *W* mutant *Wsh*, c-*kit* expression is diminished in hematopoietic progenitors in the bone marrow (BM) and lost in BM-derived mast cells (BMMCs) (5). Mastocytosis is characterized by accumulation of mast cells in various organs and release of mast cell mediators, caused by active mutations in the c-*kit* gene (6, 7). The D816V-mutated active variant of c-Kit, which is most frequently detected in patients with systemic mastocytosis, induces cluster formation and expression of several molecules involved in mast cell differentiation and adhesion, including microphthalmia transcription factor, IL-4 receptor, histamine, CD63, and ICAM-1 (8), demonstrating that c-Kit–mediated signaling is critical for differentiation and stimulation of mast cells. Therefore, determination of the mechanism of c-*kit* expression in mast cells will be useful for prevention and/or treatment of c-*kit*–mediated mast cell disorders.

The role of MITF as a transcription factor that regulates c-*kit* expression in mast cells has been extensively studied by Kitamura's group using *mi/mi* mice that carry a serious mutation in *Mitf* (9, 10). Their reports demonstrate that MITF is critical for the expression of c-*kit* in mast cells but not in erythroid precursors, testicular germ cells, or neurons. Their studies also suggest the presence of other unknown transcription factors that regulate c-*kit* expression in mast cells based on a number of observations including an increase in the proportion of c-Kit positive mast cells in *mi/mi* mice after birth.

The GATA family is comprised of six zinc-finger transcription factors, GATA1–6. Among them, GATA1, 2, and 3 are indispensable for hematopoiesis. GATA3 is considered to be essential for T cell differentiation from the earliest stages of development, and is a master regulator of Th2 differentiation (11, 12). In addition, GATA3 is upregulated by Notch2 signaling in myeloid progenitors, which facilitates development toward mast cell-producing progenitors (13). GATA1 is expressed in erythroid cells, megakaryocytes, eosinophils, and mast cells, and is involved in the development of these lineages (14–16). Furthermore, GATA1 regulates the expression of mast cell-specific molecules, including FcεRI α-, β-chains (17–20), and carboxypeptidase A genes (21). GATA2 is expressed at particularly high levels in progenitors of the several hematopoietic lineages, and is required for mast cell development but is dispensable for the terminal differentiation of erythroid cells and macrophages (22). *Gata2* knockout mice exhibit panhemapoietic defects and embryonic lethality (23), whereas enforced expression of GATA2 in mouse embryonic stem cells enhances proliferation of hematopoietic progenitors (24). In a

Atopy (Allergy) Research Center, Juntendo University School of Medicine, Tokyo, Japan

Received for publication April 15, 2010. Accepted for publication August 3, 2010.

This work was supported by a grant-in-aid for Scientific Research (C) (to C.N.) from the Ministry of Education, Culture, Sports, Science, and Technology of Japan.

Address correspondence and reprint requests to Dr. Chiharu Nishiyama, Atopy (Allergy) Research Center, Juntendo University School of Medicine, 2-1-1 Hongo, Bunkyo-ku, Tokyo 113-8421, Japan. E-mail address: chinishi@juntendo.ac.jp

Abbreviations used in this paper: BM, bone marrow; BMDC, BM-derived dendritic cell; BMMC, BM-derived mast cell; ChIP, chromatin immnoprecipitation; Ct, threshold cycle number; SCF, stem cell factor; shRNA, short hairpin RNA; siRNA, small interfering RNA.

www.jimmunol.org/cgi/doi/10.4049/jimmunol.1001228

mouse embryonic cells and OP9 stroma cell system, GATA2 not only inhibits macrophage differentiation, but also induces lineage distortion to megakaryocyte or erythroid cell differentiation by suppressing the expression and function of the transcription factor PU.1, depending on differentiation status (25). Both GATA1 and GATA2 are expressed in mast cells. Although GATA2 is dominantly expressed in immature cells (16), GATA1 is mainly expressed in mature cells. The repression of GATA1/2 leads to the impairment of cell survival, degranulation and cytokine production, due to defective signal transduction in mast cells (26, 27). These observations suggest that GATA1 and 2 play important roles in gene expression in mast cells. However, the role of GATA1 and 2 in c-*kit* expression in mast cells is largely unknown.

In the current study, we analyzed the regulation mechanisms of c-*kit* expression in mast cells and found that c-*kit* expression of mast cells is maintained by GATA2 and Sp1 recruitment to the promoter region.

Materials and Methods

Cell culture

For BMMCs, linage negative BM cells from BALB/c mice were prepared using the MACS linage negative cell preparation system (Miltenyi Biotec, Tubingen, Germany), and cultured in RPMI 1640 (Sigma-Aldrich, St Louis, MO), supplemented with FBS (10%, Sigma-Aldrich), nonessential amino acid solution (1%, Invitrogen, Carlsbad, CA), SCF (100 ng/ml, Wako Junyaku, Osaka, Japan), and IL-3 (10 ng/ml, Wako Junyaku) for at least 4 wk based on previously established methods (28, 29).

For BM-derived dendritic cells (BMDCs), BM cells from BALB/c mice were cultured in RPMI 1640, supplemented with FCS (10%), nonessential amino acid solution (1%), and 10 ng/ml GM-CSF (Peprotech, London, U.K.). After at least 10 d, we harvested the loosely adherent cells.

The PT18 mouse mast cell line was cultured in RPMI 1640, supplemented with FCS (10%) and nonessential amino acid solution (1%), and the CV1 simian kidney cell line was cultured in DMEM (Sigma-Aldrich), supplemented with FCS (10%) and nonessential amino acid solution (1%).

Plasmid constructs

The mouse c-*kit* promoter (−622/+22) was subcloned into the reporter plasmid pGL3-Basic (Promega, Madison, WI) at the XhoI/HindIII sites and deletion mutants were generated using an endonuclease/exonuclease deletion kit (Takara Bio, Otsu, Japan) in a reporter assay.

Plasmids in which several bases were replaced were generated by site-directed mutagenesis using a QuikChange II site-directed mutagenesis kit (Stratagene, La Jolla, CA) according to the manufacturer's instructions. All mutations were verified by sequencing analysis.

GATA2 open reading frame cDNA was obtained from PT18 mRNA by RT-PCR using SuperScript First-Strand synthesis system (Invitrogen) and Advantage 2 DNA polymerase (Clontech, Mountain View, CA), and Sp1 and GATA1, described in a previous study (17, 30), GATA2 was subcloned into pCR3.1 expression plasmids (Invitrogen), and the generated GATA1/pCR, GATA2/pCR, and Sp1/pCR were used to produce GATA1, GATA2, and Sp1, respectively.

EMSAs

PT18 nuclear extracts were prepared as described in our previous report (19). Binding reactions were allowed to proceed at room temperature for 15 min in 10 mM HEPES, 100 ng poly(dIdC) (Amersham Pharmacia Biotech, Piscataway, NJ), FITC-labeled probes (Invitrogen), and 5 μg nuclear extract. Abs and competitor DNA were added to the reaction mixtures before the probes. Samples were analyzed by Fluoroimager (Amersham Pharmacia Biotech) after 4% PAGE. The oligonucleotides used were mouse c-*kit* −108/−77, 5′-CCC GGG CGG GAG AAG GGA GGG GCG TGG CCA CG-3′, c-*kit* GC-box competitor of c-*kit*, −108/−77 (oligo mGC) 5′-CCC GGG CGG GAG AAG GGA GGG GAC GCG TCA CG-3′, −180/−148, 5′-GGC ACA GCG CCC CCG GGA TCA GCT TAT TGC AGC-3′, and −232/−197, 5′-CTA GGA GGA AGA GGA TCC AGG GTG AAG GGC CTG TGG-3′. The underlined nucleotides indicate the position of the GC-box motif in the oligonucleotide probe and nonlabeled oligonucleotides were used as self-competitors.

Abs against Sp1 (clone 1C6), GATA1 (clone N6), and GATA2 (clone H116) were purchased from Santa Cruz Biotechnology (Santa Cruz, CA) and isotype control mouse IgG, rabbit IgG, rat IgG, respectively, were purchased from BD Biosciences (San Diego, CA).

For in vitro transcription and translation, Sp1/pCR, GATA1/pCR, and GATA2/pCR were used with the TNT T7 Quick coupled transcription/translation system (Promega).

RNA isolation and quantitative PCR analysis

Total RNA was prepared using the RNeasy kit (Qiagen, Hilden, Germany). For quantitative analysis, cDNA synthesis was performed using the High Capacity cDNA Reverse Transcription kit (Applied Biosystems, Foster City, CA) and analyzed with a gene specific TaqMan probe (Applied Biosystems), GATA2 (Mm 00492300_m1), Sp1 (Mm 00489039_m1), and c-*kit* (Mm 00445212_m1), using the 7500 real-time PCR system (Applied Biosystems). Quantitative values were obtained from the threshold cycle number (Ct), by subtracting the average Ct of the gene from that of GAPDH (Mm9999915_g1, Applied Biosystems) and expressed as 2-ΔCt (20).

Luciferase assay

BMMCs and BMDCs (1–0.5 × 10^6 cells) were transfected with 5 μg reporter plasmid, 3 μg expression plasmid (for coexpression analysis), and 50 ng pRL-null (Promega) by electroporation using Nucleofector II (Lonza, Basel, Switzerland) using a Macrophage Kit (Lonza) and a dendritic cell Kit (Lonza) according to the manufacturer's instructions, respectively. CV1 cells (1 × 10^5) were transfected with 1 μg reporter plasmid, 200 ng expression plasmid, and 1 ng pRL-null by FuGene 6 (Roche, Indianapolis, IN) according to the manufacturer's instructions.

After 20 h, cells were harvested and the Dual-luciferase assay kit (Promega) and Micro Lumat Plus (Berthord Technologies, Bad Wildbad, Germany) were used to assess luciferase activity. Firefly luciferase activity derived from the reporter plasmid was normalized to Renilla luciferase activity derived from pRL-null.

Chromatin immunoprecipitation and rechromatin immunoprecipitation assays

Chromatin immunoprecipitation (ChIP) assays were performed as described previously (20) according to manufacturer's instructions (Upstate, Lake Placid, NY) using 1–2 × 10^6 BMMCs and PT18 cells per sample. The amounts of target DNA bound to GATA1, GATA2 or Sp1 were quantified using the 7500 real-time PCR system. The ratio of a specific DNA fragment in each immunoprecipitate to the fragment in the DNA before immunoprecipitation (input DNA) was calculated from each Ct value.

Anti-GATA1 Ab, anti-GATA2 Ab, anti-Sp1 Ab, and isotype control Abs were used the same Abs for EMSA analysis. The primer and MGB probe sequences used for this analysis were as follows: for the promoter region, c-*kit*_F (5′-CCGGGATCAGCTTATTGCA-3′), c-*kit*_R (5′-GCTACAGCTC-TCGCCCAAGT-3′), and MGB probe c-*kit*_T (5′-FAM-CAGCTCGTGGC-CAC-3′); for the cis control region, c-*kit* -*cis*C_F (5′-TCAGCTGCA-TAGTGAAGTCAACTTAG-3′), -*cis*C_R (5′-TCCAGCCTGGTCTACATA-GGAATTA-3′), and BGM probe -*cis*C_T (5′-FAM-CTACATAGCAAGA-AACTT-3′).

The re-ChIP assay was performed as described previously (31). The primary Ab-treatment was performed as for the ChIP assay, except that the conditions were scaled up. Briefly, 1 × 10^7 BMMCs were fixed in formaldehyde, lysed in cell lysis buffer, and sonicated to generate DNA fragments, to which 10 μg of the primary Ab, anti-GATA2 Ab, or isotype control rabbit IgG, was added. The immunocomplex was precipitated with protein G-agarose, was washed with various washing buffers, and was then released from the beads by incubation in the elution buffers at 37°C for 1h. The eluant of the primary immunocomplex obtained using this first Ab was diluted 10-fold with dilution buffer containing 20 mM Tris-HCl, pH 8.0, 1 mM EDTA, 150 mM NaCl, and 1% Triton X-100. A second Ab, anti-Sp1 Ab, or isotype control IgG, (10 μg each) was added to the diluted solution to obtain the secondary immunocomplex. After extraction of the immunocomplex, which was precipitated with protein G-agarose, in the same way as that for the first complex, the cross-linking between chromosome DNA and nuclear proteins was reversed. The chromosome DNA was then purified by phenol and chloroform extraction and was subjected to real-time PCR using the same primers and probe sets as used in the ChIP assay.

Flow cytometry analysis

For detection of cell surface expression of c-Kit, cells were incubated with FITC-labeled anti-Fc ε RI α-chain Ab and PE-labeled anti-mouse c-Kit Ab purchased from eBioscience (San Diego, CA) and BD Bioscience (Franklin Lakes, NJ), respectively, and analyzed using flow cytometry (FACS Calibur, BD Biosciences).

Retrovirus infection

An oligonucleotide designed to function as a short hairpin RNA (shRNA) against GATA2, (5′-GATCCCCCAAGTGCATGCAAGAGAATTCAAGAGATTCTCTTGCATGCACTTGGTTTTTA-3′), was inserted into the retroviral vector for expression of shRNA, pSUPER retro-puro (OligoEngine, Seattle, WA), and retroviral supernatants were prepared using transfection of PLAT/E packaging cells. The underlined nucleotides were required as spacers. PT18 cells were cultured in growth medium with 1 μg/ml puromycin for 10 d to obtain transfectants prior to culture in normal medium.

Western blot analysis

Cell nuclear extracts (from 1×10^6 cells) were electrophoresed through a 10% SDS polyacrylamide gel and transferred to a membrane (Immobilon-P, Millipore, Bedford, MA). The proteins on the transferred membrane were detected using the Odyssey infrared imaging system (LI-COR Biosciences, Lincoln, NE) and the density of bands analyzed. Anti-YY1 (clone H10) and anti-GATA2 Abs were purchased from Santa Cruz Biotechnology. Alexa680-conjugated anti-rabbit IgG (Invitrogen), and IRDye800-conjugated anti-mouse IgG (Rockland, Philadelphia, PA) were used as the secondary Abs.

Transfection of small interfering RNA

GATA2 small interfering RNA (siRNA) (SI01009764), Sp1 siRNA (SI1429869), and nonsilencing control siRNA (107280) were purchased from Qiagen. A 5 μl aliquot of 20 μM siRNA was added to 5×10^5 BMMCs with Nucleofector II. After 20 h of culture, GATA2, Sp1, and c-*kit* mRNA was analyzed by quantitative PCR.

Statistical analysis

We used Student unpaired two-tailed *t* test for all statistical analyses. Differences between groups were considered significant when $p < 0.05$, and indicated with a single asterisk ($p < 0.05$), double asterisks ($p < 0.01$), or triple asterisks ($p < 0.001$). All statistical analyses were performed with GraphPad Prism software (GraphPad Software, San Diego, CA).

Results

The GC-box is critical for c-kit *promoter activity*

To examine cell type-specific promoter regulation of the c-*kit* gene, we generated the reporter plasmid −622/pGL3-Basic (−622/B), by introducing the 5′-upstream region of the putative translational initiation codon of the mouse c-*kit* gene, including the 622 bp promoter and 22 bp 5′-UT (−622/+22), upstream of the luciferase gene of pGL3-Basic (Basic). Then, to screen *cis*-acting elements within the c-*kit* promoter region, three 5′-deletion constructs carrying various lengths of 5′-flanking region were generated from −622/B. The luciferase activity of BMMCs that had been transiently transfected with −232/pGL3-basic (−232/B) was ~12-fold higher than that of BMMCs transfected with Basic (Fig. 1*A*). The promoter activity was significantly reduced by the deletion of −232/−62, although the deletion of −622/−233 markedly increased the promoter activity. In contrast, c-*kit* promoter activity driven from −232/B, −61/B, and −5/B was not significantly different from that of Basic in BMDCs, in which c-Kit cell surface expression was not detected (Fig. 1*B*). These results suggest that the −232/−62 region contains the elements necessary for expression of the c-*kit* promoter, which is active only in c-Kit positive cells.

To identify the critical *cis*-enhancing elements in the −232/−62 region, we constructed various mutant promoters based on the −232/B plasmid with introduction of nucleotide replacements by site-directed mutagenesis. As shown in Fig. 2, several transcription factor binding motifs; two GATA motifs, the PU.1 motif, the GC-box, and the E-box, were found in the −232/+22 region based on motif analysis. The introduction of a GC-box mutation (mGC/B) markedly reduced the luciferase activity of −232/B, whereas mutation of PU.1 or the E-box (mPU/B or mE/B, respectively) did not affect the promoter activity of −232/B. In contrast, lacking either the GATA motif of −232GA/B or −165GA/B enhanced c-*kit* promoter activity. These results suggest that the GC-box is crucial for functioning of the c-*kit* promoter in BMMCs.

Specific binding of Sp1 to the c-kit *promoter via the GC-box*

To identify the transcription factor binding to the GC-box, EMSA was performed by using FITC-labeled double-stranded oligonucleotides as the probe (−108/−77 region) with PT18 nuclear extract in the presence or absence of the competitive oligonucleotides or Abs. The intensity of the band marked with the arrow (Fig. 3*A*, *lane 1*) was decreased by addition of anti-Sp1 Ab (Fig. 3*A*, *lane 3*), whereas isotype control IgG had no effect on this band (Fig. 3*A*, *lane 2*). When Sp1 produced by an in vitro transcription/translation system was used for EMSA, the band that showed mobility identical with that observed with the nuclear protein from PT18 was detected (Fig. 3*A*, *lane 4*) and was supershifted by addition of anti-Sp1 Ab as shown by the asterisk (Fig. 3*A*, *lane 5*). Unlabeled competitive oligonucleotides were also used to confirm the binding of Sp1 to the GC-box. The band that appeared in the mixture of probe and PT18 nuclear extract disappeared by addition of the self-competitor (Fig. 3*A*, *lane 6*). In contrast, mutant competitor lacking the GC-box (oligo mGC) had no effect on this band, (Fig. 3*A*, *lane 7*). Similarly, the band caused by addition of in vitro Sp1 disappeared in the presence of self-competitor (Fig. 3*A*, *lane 8*), but remained in the presence of the oligo mGC competitor (Fig. 3*A*, *lane 9*). These results indicate that the transcription factor Sp1 binds to the GC-box of the c-*kit* promoter.

To examine the possibility that GATA1 and/or GATA2 bind to two GATA motifs in the −232/B reporter plasmid, we performed EMSA as shown in Fig. 3*B*. Both GATA1 and GATA2 proteins, which were produced using an in vitro transcription/translation system, bound to the −232/−197 and −180/−148 probes, and bands with GATA proteins and probes disappeared in the presence of anti-GATA1 or anti-GATA2 Ab. These findings suggest that both GATA1 and GATA2 may be recruited to GATA motifs.

To further investigate whether GATA factors and Sp1 bind to the c-*kit* promoter in vivo, a ChIP assay was performed using BMMCs and BMDCs (Fig. 4). A markedly higher amount of chromatin-containing c-*kit* promoter region (−168/+22) was immunoprecipitated by anti-GATA2 Ab (Fig. 4*A*) compared with control IgG in BMMCs, whereas significant binding of GATA2 was not detected in BMDCs (Fig. 4*C*). In addition, a significantly higher amount of c-*kit* promoter region was detected in the immunoprecipitant produced by anti-Sp1 Ab compared with isotype control IgG in BMMCs (Fig. 4*A*), but not in BMDCs (Fig. 4*C*). In contrast, a significant difference was not detected between anti-GATA1 and isotype control IgG in either BMMCs or BMDCs. Anti-GATA1 Ab, anti-GATA2 Ab, and anti-Sp1 Ab in both BMMCs and BMDCs did not immunoprecipitate the *cis*-control region of the c-*kit* promoter (Fig. 4*B*, 4*D*). These results suggest that GATA2 and Sp1, but not GATA1, are recruited to the c-*kit* promoter in a BMMC-specific manner.

The GC-box is essential for GATA2-mediated transactivation of the c-kit *promoter*

Furthermore, to elucidate the function of GATA1, GATA2, and Sp1 in the c-*kit* promoter, we introduced the GATA1/pCR, GATA2/pCR , or Sp1/pCR expression plasmid with various mutant plasmids based on −232/B into CV1 cells, and determined luciferase activity. As shown in Fig. 5*A*, each of the mutant reporter plasmids, lacked the GATA and/or the GC-box motifs by nucleotides replacement, was used for coexpression analysis. Enforced expression of GATA2 additionally enhanced the luciferase activities of −232/B and *m*-222,165GA/B to ~4-fold that of empty

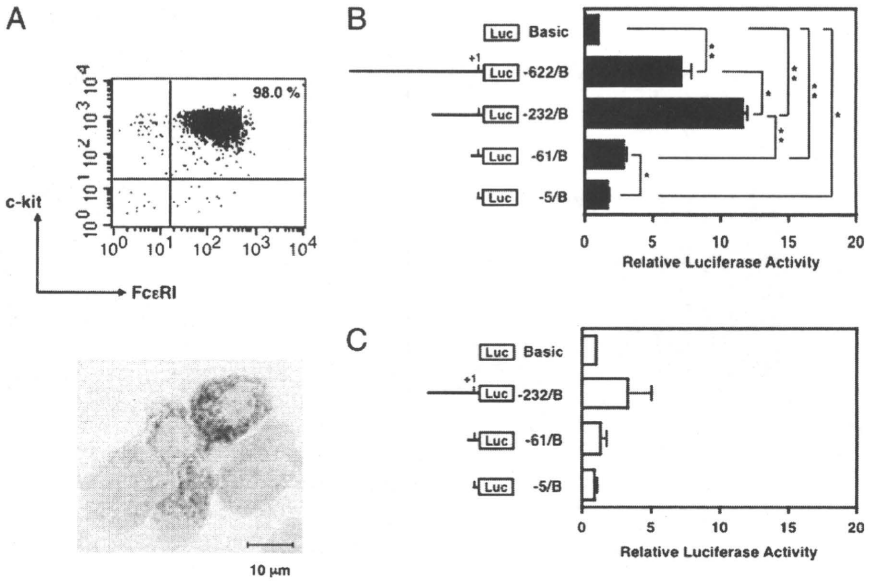

FIGURE 1. c-*kit* promoter activity was reduced by deletion between −232/−62 in BMMCs. *A*, Surface expression of c-Kit and FcεRI, and staining with Alcian blue (original magnification ×630) of BMMCs used in the current study. *B* and *C*, The 5 μg amount of each reporter plasmid was introduced into BMMCs (*B*) or BMDCs (*C*) by electroporation. The relative luciferase activity driven by −622/pGL3-Basic (−622/B), −232/pGL3-Basic (−232/B), −108/pGL3-Basic (−108/B), −61/pGL3-Basic (−61/B), and −5/pGL3-Basic (−5/B) are represented as the ratio to the activity driven by pGL3-Basic (Basic). Luciferase activities were normalized to the activity of pRL-null. Each experiment was conducted in duplicate for each sample, and the results expressed as the mean ± SEM for more than three independent experiments in Figs. 1, 2, and 5.

expression plasmid, but not that of mGC/B and mGA,GC/B, whereas enforced expression of GATA1 did not affect the luciferase activities derived from CV1 cells transfected with any reporter plasmids. Interestingly, overexpression of Sp1, which was identified to bind the GC-box, did not affect any luciferase activities. In addition, we introduced GATA2/pCR expression plasmid with the mutant plasmid into BMMCs by electroporation, and the luciferase activity was determined to evaluate the effect of GATA2 on the c-*kit* promoter in mast cells (Fig. 5*B*). The luciferase activities derived from BMMCs transfected by the plasmids, −232/B and −222,165GA/B, were increased to ~2-fold by GATA2 coexpression, whereas the promoter lacking GC-box (mGC/B and mGA, GC/B) was not significantly activated. To clarify whether GATA2 interact directly to c-*kit* promoter via Sp1 of GC-box, we performed EMSA using FITC-labeled probe containing GC-box motif (−108/−77) and in vitro translated Sp1 and GATA2 (Fig. 5*C*). When Sp1 and GATA2 were added to the probe after incubation at room temperature, the band marked with an asterisk appeared (*lane 2*) with lower mobility shift than that of the band containing Sp1 and the probe shown with the arrow (*lane 1*), suggesting that the m.w. of the complex marked with an asterisk is higher compared with that of Sp1 and probe. In addition, this band with lower mobility was supershiftred by addition of anti-Sp1 as shown with double asterisks (*lane 5*) with showing higher m.w. than that of probe/Sp1/anti-Sp1 Ab complex as marked with an arrowhead with an asterisk (*lane 4*). In contrast, the band by addition of GATA2 alone to the probe mixture did not cause the specific band shift (*lane 3*). These results suggest that GATA2 transactivates the c-*kit* promoter via GC-box *cis*-element, and that GATA2 binds the GC-box in the presence of Sp1.

To further confirm the interaction between GATA2 and Sp1 on the c-*kit* promoter in the BMMC chromosome, we performed a re-ChIP assay. The results of this assay indicate that GATA2 and Sp1 are simultaneously recruited to a region, including GC-box of the c-*kit* promoter, but not to a control region (Fig. 5*D*).

c-kit *expression was reduced by knockdown of GATA2 and/or Sp1*

Although a transactivating function of GATA2 was found in the coexpressing reporter assay, no effect of exogenous Sp1 was observed in the assay, which may have been due to the endogenous Sp1. Therefore, to further confirm the necessity of GATA2 and Sp1 for c-*kit* expression in BMMCs, GATA2, and/or Sp1 siRNA were introduced by electroporation. The c-*kit* mRNA levels in the resultant transfectants were determined using quantitative real-time PCR after 20 h cultivation (Fig. 6*A–C*), and binding of GATA2 and/or Sp1 to the c-*kit* promoter was analyzed by ChIP analysis (Fig. 6*D–G*). The GATA2 mRNA level in the GATA2 siRNA transfectants siGATA2/BMMC (GATA2 in Fig. 6*A*), and the Sp1 mRNA level in the Sp1 siRNA transfectants Sp1 siRNA (siSp1)/BMMC (Sp1 in Fig. 6*B*), were reduced by ~20 and 15%, respectively, whereas transfection of GATA2 siRNA and Sp1 siRNA had little effect on the mRNA levels of the other. The mRNA levels of c-*kit* in BMMCs were decreased to 40 or 60% by knockdown of GATA2 or Sp1, respectively (c-*kit* in Fig. 6*A*, 6*B*). These data indicate that a decrease in either GATA2 or Sp1

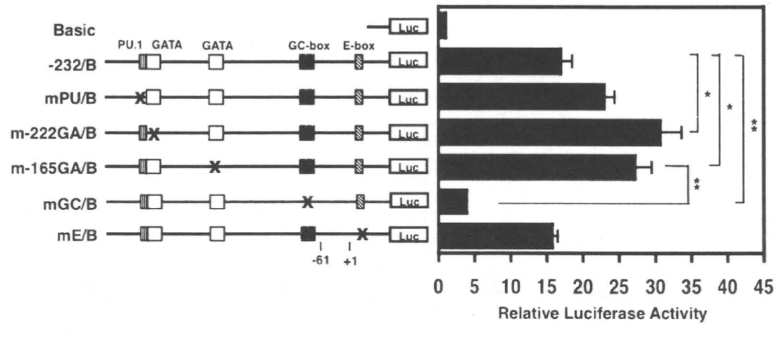

FIGURE 2. Mutation of the GC-box impaired c-*kit* promoter activity. BMMCs were transfected with 5 μg of each reporter plasmid, Basic, −232/B, or the mutated −232/B constructs produced by nucleotide replacement (shown as × here and in Fig. 5). The relative luciferase activity is represented as the ratio to the activity driven by pGL3-Basic (Basic).

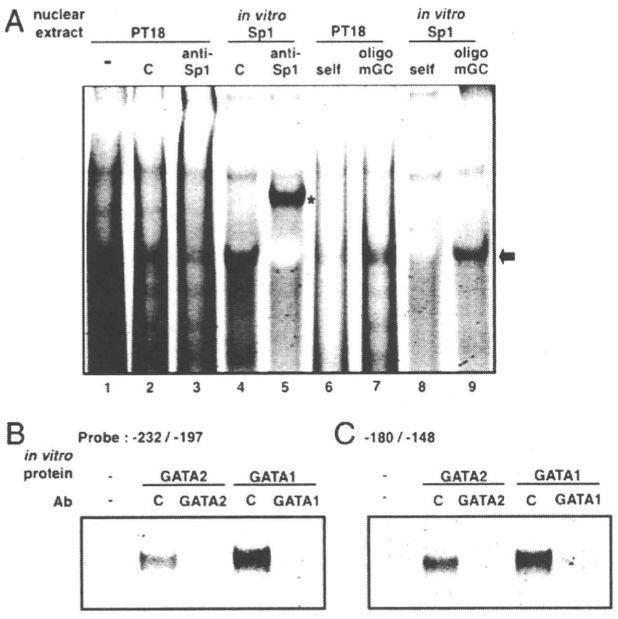

FIGURE 3. Sp1 and GATA1 and/or GATA2 are recruited to the −107/−77 region, and −232/−197 and −180/−148 region, respectively. *A*, EMSAs were performed with the use of 5 pmol FITC-labeled probe, 5 μg of PT18 cell nuclear extract, and in vitro translated Sp1. The arrow indicates the position of the specific band containing probe and Sp1. *Lanes 1–3, 6,* and *7*, Labeled probe and PT18 nuclear extract; *lanes 4, 5, 8* and *9*, labeled probe and in vitro translated Sp1. Additives: *lane 1*, none (−); *lane 2*, isotype control IgG (C); *lane 3*, anti-Sp1 Ab; *lane 4*, isotype control IgG (C); *lane 5*, anti-Sp1 Ab; *lanes 6* and *8*, nonlabeled probe (self); *lanes 7* and *9*, nonlabeled oligonucleotides containing mutated GC-box sequences introduced by nucleotide replacement (oligo mGC). Asterisk indicates the position of the supershifted band containing probe, in vitro translated Sp1 and anti-Sp1 Ab. *B*, GATA1 and GATA2 protein, prepared by an in vitro transcription/translation system, were incubated with 5 pmol of −232/−197 or −180/−148 FITC labeled probes and anti-GATA1 Ab, anti-GATA2 Ab, or isotype control IgG (C).

expression impairs the promoter activity of c-*kit*. Cotransfection of GATA2 siRNA and Sp1 siRNA into BMMCs, which reduced the mRNA levels of GATA2 and Sp1 to the same degree as mentioned above for single siRNA usage, downregulated the mRNA of c-*kit* by ~50% (Fig. 6*C*). To confirm whether the recruitment of GATA2 and/or Sp1 to the c-*kit* promoter region was reduced in siRNA-transfected BMMCs, a ChIP assay was performed after 20 h cultivation following siRNA transfection. As shown in Fig. 6*D*, binding of GATA2 to the c-*kit* promoter was not detected in BMMCs transfected with GATA2 siRNA (siGATA2) (siGATA2/BMMC), and the amount of GATA2 binding to the c-*kit* promoter in Sp1 siRNA-transfected BMMCs (siSp1/BMMC) was ~20% of that in nonsilencing control siRNA-transfected BMMCs (siNega/BMMC). The binding of Sp1 to the c-*kit* promoter disappeared in siSp1/BMMCs, whereas the amount of Sp1 detected in siGATA2/BMMC was almost the same level as that of siNega/BMMC (Fig. 6*F*). The promoter-specific binding of the transcription factors was confirmed by the *cis*-control ChIP assay (Fig. 6*E*, 6*G*). These findings suggest that the recruitment of Sp1 to the promoter region of c-*kit* is necessary for the binding of GATA2.

Repression of GATA2 expression by shRNA resulted in a decrease in the surface expression of c-kit *in PT18*

To further investigate the necessity of GATA2 for c-*kit* expression, GATA2 expression was knocked down in the mouse mast cell line PT18 by introduction of GATA2 shRNA/pSuper (shGATA2/PT18). PT18 cells were used for this experiment instead of BMMCs because 10 d culture of BMMCs under GATA2 knockdown condition (resulting in suppression of c-*kit* expression) to obtain shGATA2-transfectants may affect the viability and/or survival of BMMCs, which are depend on c-Kit ligand SCF, whereas PT18 are growing in SCF-independent manner. After 10 d of culture in growth medium containing puromycin to select transfectants, cells were harvested, and analyzed by flow cytometry. Surface c-Kit expression of shGATA2/PT18 was approximately one tenth lower than that obtained by transfection of empty vector (mock/PT18) (Fig. 7*A*). Densitometry analysis of Western blotting demonstrated that the amount of GATA2 protein in shGATA2/PT18 was reduced to ~20% of that in mock/PT18 (Fig. 7*B*), whereas the protein levels of the ubiquitously expressed transcription factor YY-1 was comparable between both transfectants. The ChIP assay showed that the recruitment of GATA2 to the c-*kit* promoter (−168/+22) was reduced in shGATA2/PT18 (Fig. 7*C*). A significant difference was not detected between anti-GATA2 and isotype control IgG in the *cis*-control region of shGATA2/PT18 and mock/PT18 (Fig. 7*D*). These results suggest that GATA2 is essential for the cell-surface expression of c-Kit in mast cells.

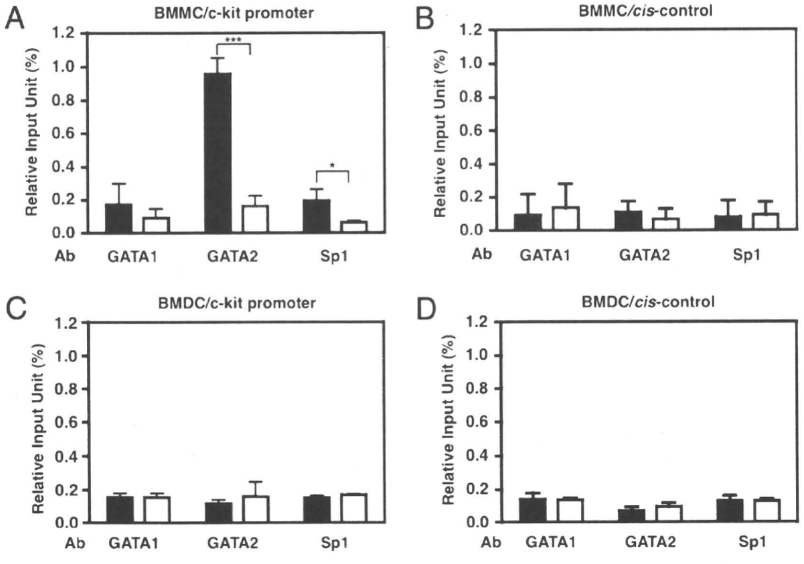

FIGURE 4. GATA2 and Sp1 are recruited to the c-*kit* promoter in mast cells. In BMMCs (*A*, *B*) and BMDCs (*C*, *D*), quantitative analysis of Sp1 and GATA binding to the c-*kit* gene by the ChIP assay using real-time PCR was performed. The closed box indicates anti-GATA1, anti-GATA2, or anti-Sp1 Abs and the open box indicates isotype control IgG. *A* and *C* show the results of PCR with a c-*kit* specific probe, and (*B*) and (*D*) show that with a *cis*-control probe. The results express the mean ± SEM for two PCR with duplicate samples in each of three independent ChIP assays. Relative input units are calculated from Ct values as described in the ChIP assay method.

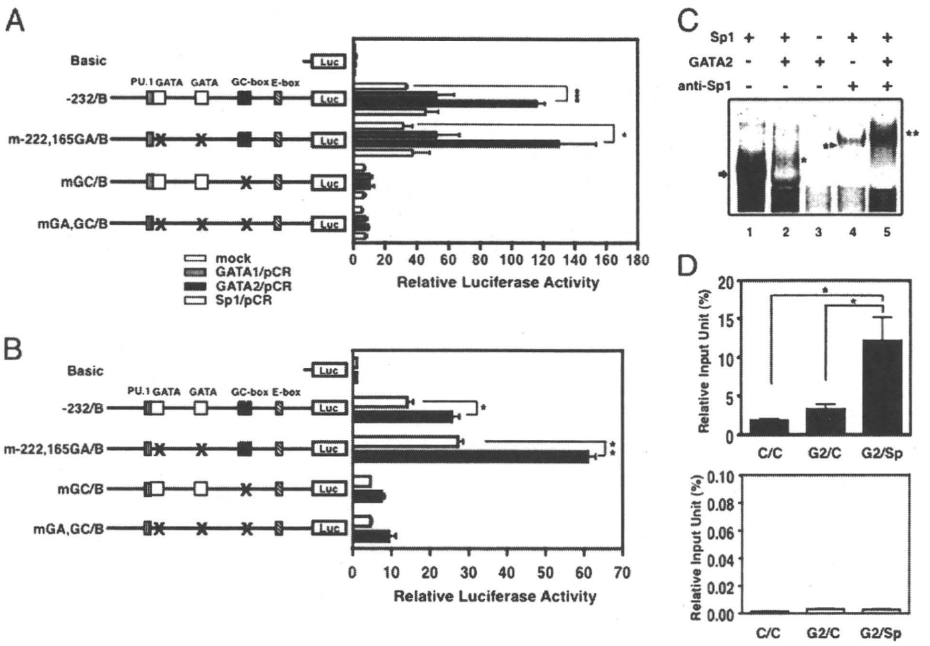

FIGURE 5. The luciferase activity of the c-*kit* promoter was enhanced by GATA2 coexpression in CV1 cells. *A*, A 1 μg amount of each reporter plasmid and 100 ng of expression plasmid were introduced into CV1 cells using FuGene 6. The relative luciferase activity is represented as the ratio to the activity driven by pGL3-Basic (Basic) and pCR3 empty vector (mock). *B*, BMMCs were transfected 5 μg each of reporter plasmids and 3 μg of expression plasmid (pCR3 empty plasmid, open box, or GATA2/pCR, closed box) by electroporation. The ratio of luciferase activity of each construct to that of Basic in the presence of empty expression plasmid was represented as relative luciferase activity. *C*, EMSAs were performed with the use of 5 pmol FITC-labeled probe (−108/−77) and in vitro translated Sp1 and/or GATA2. The arrow indicated the position of the band containing Sp1 and the probe, and the asterisk indicated that of the band containing Sp1, GATA2, and the probe. *Lane 1, 2, 4,* and *5*, In vitro translated Sp1; *lane 2, 3,* and *5*, in vitro translated GATA2; *lane 4* and *5*, anti-Sp1 Ab. Double asterisks indicated the position of supershifted band containing in vitro translated Sp1, GATA2, the probe, and anti-Sp1 Ab. *D*, Re-ChIP analysis. C, isotype control IgG; G2, anti-GATA2 Ab; Sp, anti-Sp1 Ab. The result of PCR using a c-*kit* specific probe (*top*) or a *cis*-contol probe (*bottom*), are shown. The results are expressed as the mean ± SEM for two PCR reactions, with duplicate samples, in each of three independent re-ChIP assays. Relative input units are calculated from the Ct values as described in the ChIP assay method.

Discussion

Although the molecular bases for the transcriptional regulation of c-*kit* in hematopoietic stem cells have been investigated, the mechanisms of c-*kit* transcription in mast cells, which continuously express c-*kit* at a high level, have been unclear. Thus, we investigated c-*kit* transcriptional regulation in mast cells using a reporter assay, EMSA, and a ChIP assay with an RNA interface. In this study, we demonstrated that the transcription factors GATA2 and Sp1 maintain c-*kit* expression cooperatively.

In the reporter assay using a series of 5′- deletion promoter constructs, the mouse c-*kit* promoter was functional only in BMMCs, but not in BMDCs, as shown in Fig. 1, indicating that cell type-specific promoter activity is assigned within the −232/−62 promoter region. Motif analysis using the program TFSEACH (http://www.cbrc.jp/reseach/db/TFSEACH.html) revealed the presence of one PU.1-binding motif, two GATA-binding motifs, one GC-box, and one E-box in the −232/+22 region. These motifs were candidates for *cis*-enhancing elements for the following reasons. GATA and SCL, which binds to the E-box, are predominantly expressed in hematopoietic cells, and the pentameric complex, containing GATA, SCL, E2A, LMO2, and Ldb-1, bind to DNA via the GATA or SCL/E2A or Sp1 motif, either alone or in combination (32, 33). GATA and PU.1 are essential for the generation of mast cells (34). Our reporter assay using various mutated constructs revealed that the GC-box is the essential element for functioning of the c-*kit* promoter (Fig. 2). By EMSA using anti-Sp1 Ab and competitive oligonucleotides, Sp1 was identified to bind the GC-box in the −108/−77 region (Fig. 3*A*). In addition, GATA1 and/or GATA2 possess the ability to bind to two GATA motifs in −232/B by EMSA (Fig. 3*B*). In the ChIP assay, we detected significant binding of Sp1 and GATA2 to the −232/−62 region of the c-*kit* promoter, but GATA1 binding was not observed in BMMCs (Fig. 4*A*). These findings suggest that both Sp1 and GATA2 are recruited to the c-*kit* promoter region and activate the promoter in BMMCs in a cell type-specific manner (Fig. 4*C*). GATA has been shown to bind (A/T)GATA(A/G) or GATC sequences directly (35), and other studies have shown that the activity of GATA protein is modulated by interaction with other factors as follows. In erythrocytes, the complex of GATA1 and cofactor FOG1 coordinates cell maturation, and GATA1 represses activation of erythroid-specific gene expression by direct binding of NuRD/MeCP1 complex to FOG1 (36, 37). In megakaryocytes, the interaction of GATA1 and the SCL complex, which includes SCL, E2A, Ldb1, LMO2, and ETO2 regulate cell maturation (38). In mast cells, recruitment of FOG1 toward GATA1 represses the expression of the FcεRI β-chain, which allows mast cell-specific expression of the β-chain (20). In the current study, the E-box did not contribute to c-*kit* promoter function, suggesting that SCL is possibly not involved in c-*kit* promoter functions. In addition, we did not detect significant recruitment of FOG1 toward the c-*kit* promoter in the ChIP assay (data not shown). Previously, Tsujimura et al. (10) showed that MITF transactivates the c-*kit* promoter via binding to the CACCTG motif at −356/−351. However, in the current study, deletion of −622/−233 significantly increased c-*kit* promoter activity (Fig. 1). Although we do not have evidence to explain this discrepancy, one possible reason for the different results may be that different host cells were used for the reporter assay. In the previous studies, the cell lines, FMA3 and FDC-P1 were used for the reporter assay without exogenous MITF, and

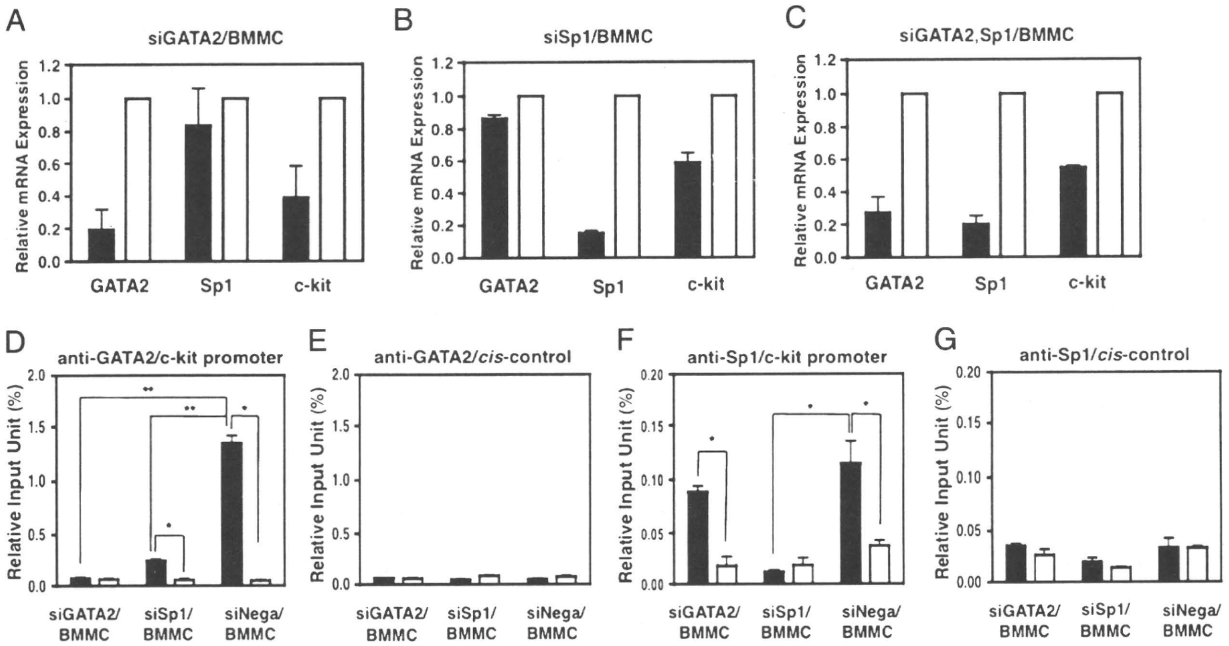

FIGURE 6. Transfection of GATA2 and/or Sp1 siRNA induced c-*kit* mRNA repression in BMMCs. *A–C*, Quantification of GATA2, Sp1, and c-*kit* mRNA in siRNA transfectants, siGATA2/BMMC (*A*), siSp1/BMMC (*B*), and siGATA2, Sp1/BMMC (*C*), using real-time PCR. The relative mRNA expression levels of siRNA transfectants (closed box) are represented as the ratio to that of control siRNA transfectants (open box). *D–G*, siRNA transfectants (siGATA2/BMMC, siSp1/BMMC, and siNega/BMMC) were analyzed with anti-GATA2 Ab (*D*, *E*) or anti-Sp1 Ab (*F*, *G*) in a ChIP assay. The amount of c-*kit* specific promoter (*D*, *F*) or *cis*-control (*E*, *G*) in each immunoprecipitate was quantified by real-time PCR. The closed box indicates the relative input unit by anti-GATA2 or anti-Sp1 Abs and the open box indicates that by isotype control IgG.

NIH/3T3 was used for the MITF-coexpression reporter assay (10), whereas BMMCs were used in the present reporter assay with deletion construct (Fig. 1). Considering that CACCTG functions as a *cis*-enhancing element in a mastcytoma, but not in another myeloid cell line, the effect of MITF may be differentially controlled in a cell type-specific manner. Furthermore, the function of MITF in BMMCs at various developmental stages may be different from its function in mast cell line. Alternatively, it is possible that an element in some other region of −622/−233 might affect the function of MITF. Such an element would be lost in the −622/−233 deletion mutant in the current study but would be retained in the point mutation of CACCTG in the previous study. In our preliminary experiments, MITF was associated with the complex containing GATA2 and chromosome in the re-ChIP assay (data not shown). Further detailed analysis will be required to clarify the complicated roles of each transcription in the function of the c-*kit* promoter.

To identify the mechanisms of the enhancement of c-*kit* promoter activity by GATA2 and Sp1, we performed a reporter assay using various reporter constructs, introduced nucleotide replacements in the GATA and/or Sp1 binding motifs, and GATA2 or Sp1 expression plasmids, and EMSA using in vitro translated Sp1 and GATA2 (Fig. 5). In both of CV1 cells and BMMCs, the reporter activities of the wild-type c-*kit* promoter (−232/B) were enhanced by cotransfection with GATA2 expression plasmid. Although the reporter activity of −232/B and *m*-222,165GA/B were not enhanced by coexpression of Sp1 in CV1 cells, this unexpected result may

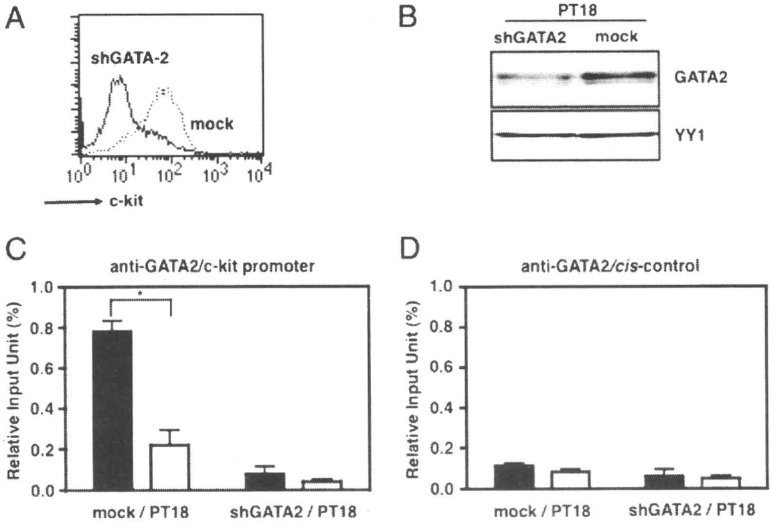

FIGURE 7. Expression of shGATA2 induced the downregulation of c-*kit* transcription and surface expression in PT18. *A*, Surface expression of c-Kit on shGATA2 transfectants. PT18 cells transfected with shGATA2/pSuper-retro-puro (shGATA2, solid line) or empty vector (mock, dotted line) were stained with PE-conjugated anti–c-Kit Ab. *B*, Western blot analysis of shGATA2-transfected PT18 cells. Cells were transfected with shGATA2 or empty vector and cultured in the presence of puromycin for at least 10 d. Cell lysates (1×10^6 cells per lane) were analyzed using anti-GATA2 or anti-YY1 Ab. *C* and *D*, Quantitative analysis of GATA2 binding to the c-*kit* promoter in a ChIP assay using real-time PCR. Chromatin of transfected PT18 cells was immunoprecipitated by anti-GATA2 Ab or isotype control IgG. Precipitated DNA molecules were analyzed by real-time PCR to test for the presence of the c-*kit* promoter (*C*) or the *cis*-control locus (*D*). The open box indicates isotype control IgG and the closed box indicates anti-GATA2 Ab.

have been due to the endogenous expression of Sp1 in CV1 cells. Regardless, coexpression analysis with CV1 indicated that GATA2 transactivates the c-*kit* promoter via the GC-box, independent of the SCL complex (33), because the hematopoietic specific factors, SCL and LMO2, are not expressed in CV1 cells. By EMSA using in vitro translated Sp1 and/or GATA2, GATA2 is suggested to the GC-box in the presence of Sp1, whereas GATA2 alone cannot bind the GC-box. Although the band containing Sp1 and GATA2 was not detected when EMSA was performed using PT18 nuclear extract and the same probe in Fig. 3*A*, this may have been due to dissociation of Sp1 and GATA2 during nuclear extraction, because the re-ChIP assay suggests that Sp1 and GATA2 are simultaneously recruited to the GC-box site in the c-*kit* promoter.

Mutant promoters lacking GATA motifs exhibited higher transcriptional activity compared with that of wild-type in mast cells (Fig. 2). One of the hypotheses of this enhancement may be that mutation of GATA-motif in the promoter, which plays a competitive role against the GC-box in the recruitment of GATA2, increased the amount of GATA2 binding to Sp1 on the GC-box. Alternatively, these GATA-motifs may function as silencing elements that suppress the c-*kit* promoter in other GATA1/2 positive hematopoietic lineage, including erythroids and megakaryocytes. Further analysis of GATA1/2 profiles on these GATA-motifs in various cell-types may provide interesting information regarding the mechanism of cell type-specific c-*kit* expression.

By knockdown of GATA2 and/or Sp1 in BMMCs, c-*kit* mRNA expression was reduced to ~50% (Fig. 6*A–C*), and GATA2 recruitment to the promoter region was reduced by the impaired recruitment of Sp1 in the ChIP assay (Fig. 6*D–G*). Furthermore, c-Kit surface expression of PT18 was reduced by GATA2 knockdown, accompanied with decreased recruitment of GATA2 to the promoter region (Fig. 7). These results indicate that the recruitment of GATA2 and Sp1 to the GC-box mainly enhances the c-*kit* promoter. The c-*kit* mutant promoters lacking GATA motifs was transactivated by GATA2 in the current study, suggesting that GATA2 is involved in c-*kit* promoter function without binding to the GATA motifs, although these GATA motifs possess GATA protein binding affinity. One of the possible mechanisms is indirect interaction with the GC-box via the formation of a complex with Sp1. The ChIP assay with siRNA-transfected BMMCs showed that the recruitment of GATA2 to the c-*kit* promoter is dependent on the presence of Sp1. In addition, the re-ChIP assay showed that both Sp1 and GATA2 are specifically recruited to the region of the GC-box. These data suggest that GATA2 binds to the GC-box via Sp1 binding, and that formation of a complex accelerates the binding of Sp1 to the GC-box. Sp1 physically interacts with GATA1, 2, and 3 and functions as a scaffold for GATA1 binding to the globin gene,-which lacks GATA motifs (39). In addition, GATA3 regulates the dopamine β-hydroxylase gene through physical interaction with Sp1 (40). These observations support our hypothesis that GATA2 regulates the expression of the c-*kit* gene by interaction with Sp1. In any case, our data indicate that GATA2 interacts with the c-*kit* promoter region via Sp1 and maintains expression of the c-*kit* gene in a mast-cell-specific manner, although further analysis is required to clarify the involvement of other transcription factors.

Acknowledgments

We thank the members of the Atopy (Allergy) Research Center and the Department of Immunology for helpful discussions. We also thank Dr. Hiroko Ushio for useful advice, Mutsuko Hara and Tomoko Tokura for technical support, and Michiyo Matsumoto for secretarial assistance.

Disclosures

The authors have no financial conflicts of interest.

References

1. Chen, C. C., M. A. Grimbaldeston, M. Tsai, I. L. Weissman, and S. J. Galli. 2005. Identification of mast cell progenitors in adult mice. *Proc. Natl. Acad. Sci. USA* 102: 11408–11413.
2. Arinobu, Y., H. Iwasaki, M. F. Gurish, S. Mizuno, H. Shigematsu, H. Ozawa, D. G. Tenen, K. F. Austen, and K. Akashi. 2005. Developmental checkpoints of the basophil/mast cell lineages in adult murine hematopoiesis. *Proc. Natl. Acad. Sci. USA* 102: 18105–18110.
3. Chabot, B., D. A. Stephenson, V. M. Chapman, P. Besmer, and A. Bernstein. 1988. The proto-oncogene c-kit encoding a transmembrane tyrosine kinase receptor maps to the mouse W locus. *Nature* 335: 88–89.
4. Copeland, N. G., D. J. Gilbert, B. C. Cho, P. J. Donovan, N. A. Jenkins, D. Cosman, D. Anderson, S. D. Lyman, and D. E. Williams. 1990. Mast cell growth factor maps near the steel locus on mouse chromosome 10 and is deleted in a number of steel alleles. *Cell* 63: 175–183.
5. Duttlinger, R., K. Manova, T. Y. Chu, C. Gyssler, A. D. Zelenetz, R. F. Bachvarova, and P. Besmer. 1993. W-sash affects positive and negative elements controlling c-kit expression: ectopic c-Kit expression at sites of kit-ligand expression affects melanogenesis. *Development* 118: 705–717.
6. Zappulla, J. P., P. Dubreuil, S. Desbois, S. Létard, N. B. Hamouda, M. Daëron, G. Delsol, M. Arock, and R. S. Liblau. 2005. Mastocytosis in mice expressing human Kit receptor with the activating Asp816Val mutation. *J. Exp. Med.* 202: 1635–1641.
7. Garcia-Montero, A. C., M. Jara-Acevedo, C. Teodosio, M. L. Sanchez, R. Nunez, A. Prados, I. Aldanondo, L. Sanchez, M. Dominguez, L. M. Botana, et al. 2006. KIT mutation in mast cells and other bone marrow hematopoietic cell lineages in systemic mast cell disorders: a prospective study of the Spanish Network on Mastocytosis (REMA) in a series of 113 patients. *Blood* 108: 2366–2372.
8. Mayerhofer, M., K. V. Gleixner, A. Hoelbl, S. Florian, G. Hoermann, K. J. Aichberger, M. Bilban, H. Esterbauer, M. T. Krauth, W. R. Sperr, et al. 2008. Unique effects of KIT D816V in BaF3 cells: induction of cluster formation, histamine synthesis, and early mast cell differentiation antigens. *J. Immunol.* 180: 5466–5476.
9. Isozaki, K., T. Tsujimura, S. Nomura, E. Morii, U. Koshimizu, Y. Nishimune, and Y. Kitamura. 1994. Cell type-specific deficiency of c-kit gene expression in mutant mice of mi/mi genotype. *Am. J. Pathol.* 145: 827–836.
10. Tsujimura, T., E. Morii, M. Nozaki, K. Hashimoto, Y. Moriyama, K. Takebayashi, T. Kondo, Y. Kanakura, and Y. Kitamura. 1996. Involvement of transcription factor encoded by the mi locus in the expression of c-kit receptor tyrosine kinase in cultured mast cells of mice. *Blood* 88: 1225–1233.
11. Ting, C. N., M. C. Olson, K. P. Barton, and J. M. Leiden. 1996. Transcription factor GATA-3 is required for development of the T-cell lineage. *Nature* 384: 474–478.
12. Zhu, J., H. Yamane, J. Cote-Sierra, L. Guo, and W. E. Paul. 2006. GATA-3 promotes Th2 responses through three different mechanisms: induction of Th2 cytokine production, selective growth of Th2 cells and inhibition of Th1 cell-specific factors. *Cell Res.* 16: 3–10.
13. Sakata-Yanagimoto, M., E. Nakagami-Yamaguchi, T. Saito, K. Kumano, K. Yasutomo, S. Ogawa, M. Kurokawa, and S. Chiba. 2008. Coordinated regulation of transcription factors through Notch2 is an important mediator of mast cell fate. *Proc. Natl. Acad. Sci. USA* 105: 7839–7844.
14. Pevny, L., C. S. Lin, V. D'Agati, M. C. Simon, S. H. Orkin, and F. Costantini. 1995. Development of hematopoietic cells lacking transcription factor GATA-1. *Development* 121: 163–172.
15. Yamamoto, M., S. Takahashi, K. Onodera, Y. Muraosa, and J. D. Engel. 1997. Upstream and downstream of erythroid transcription factor GATA-1. *Genes Cells* 2: 107–115.
16. Harigae, H., S. Takahashi, N. Suwabe, H. Ohtsu, L. Gu, Z. Yang, F. Y. Tsai, Y. Kitamura, J. D. Engel, and M. Yamamoto. 1998. Differential roles of GATA-1 and GATA-2 in growth and differentiation of mast cells. *Genes Cells* 3: 39–50.
17. Nishiyama, C., T. Yokota, K. Okumura, and C. Ra. 1999. The transcription factors Elf-1 and GATA-1 bind to cell-specific enhancer elements of human high-affinity IgE receptor alpha-chain gene. *J. Immunol.* 163: 623–630.
18. Nishiyama, C., M. Hasegawa, M. Nishiyama, K. Takahashi, Y. Akizawa, T. Yokota, K. Okumura, H. Ogawa, and C. Ra. 2002. Regulation of human Fc epsilon RI alpha-chain gene expression by multiple transcription factors. *J. Immunol.* 168: 4546–4552.
19. Maeda, K., C. Nishiyama, T. Tokura, Y. Akizawa, M. Nishiyama, H. Ogawa, K. Okumura, and C. Ra. 2003. Regulation of cell type-specific mouse Fc epsilon RI beta-chain gene expression by GATA-1 via four GATA motifs in the promoter. *J. Immunol.* 170: 334–340.
20. Maeda, K., C. Nishiyama, T. Tokura, H. Nakano, S. Kanada, M. Nishiyama, K. Okumura, and H. Ogawa. 2006. FOG-1 represses GATA-1-dependent FcepsilonRI beta-chain transcription: transcriptional mechanism of mast-cell-specific gene expression in mice. *Blood* 108: 262–269.
21. Zon, L. I., M. F. Gurish, R. L. Stevens, C. Mather, D. S. Reynolds, K. F. Austen, and S. H. Orkin. 1991. GATA-binding transcription factors in mast cells regulate the promoter of the mast cell carboxypeptidase A gene. *J. Biol. Chem.* 266: 22948–22953.
22. Tsai, F. Y., and S. H. Orkin. 1997. Transcription factor GATA-2 is required for proliferation/survival of early hematopoietic cells and mast cell formation, but not for erythroid and myeloid terminal differentiation. *Blood* 89: 3636–3643.
23. Tsai, F. Y., G. Keller, F. C. Kuo, M. Weiss, J. Chen, M. Rosenblatt, F. W. Alt, and S. H. Orkin. 1994. An early haematopoietic defect in mice lacking the transcription factor GATA-2. *Nature* 371: 221–226.

24. Kitajima, K., M. Masuhara, T. Era, T. Enver, and T. Nakano. 2002. GATA-2 and GATA-2/ER display opposing activities in the development and differentiation of blood progenitors. *EMBO J.* 21: 3060–3069.
25. Kitajima, K., M. Tanaka, J. Zheng, H. Yen, A. Sato, D. Sugiyama, H. Umehara, E. Sakai, and T. Nakano. 2006. Redirecting differentiation of hematopoietic progenitors by a transcription factor, GATA-2. *Blood* 107: 1857–1863.
26. Masuda, A., K. Hashimoto, T. Yokoi, T. Doi, T. Kodama, H. Kume, K. Ohno, and T. Matsuguchi. 2007. Essential role of GATA transcriptional factors in the activation of mast cells. *J. Immunol.* 178: 360–368.
27. Nishiyama, C., T. Ito, M. Nishiyama, S. Masaki, K. Maeda, N. Nakano, W. Ng, K. Fukuyama, M. Yamamoto, K. Okumura, and H. Ogawa. 2005. GATA-1 is required for expression of FcepsilonRI on mast cells: analysis of mast cells derived from GATA-1 knockdown mouse bone marrow. *Int. Immunol.* 17: 847–856.
28. Razin, E., C. Cordon-Cardo, and R. A. Good. 1981. Growth of a pure population of mouse mast cells in vitro with conditioned medium derived from concanavalin A-stimulated splenocytes. *Proc. Natl. Acad. Sci. USA* 78: 2559–2561.
29. Razin, E., J. N. Ihle, D. Seldin, J. M. Mencia-Huerta, H. R. Katz, P. A. LeBlanc, A. Hein, J. P. Caulfield, K. F. Austen, and R. L. Stevens. 1984. Interleukin 3: A differentiation and growth factor for the mouse mast cell that contains chondroitin sulfate E proteoglycan. *J. Immunol.* 132: 1479–1486.
30. Kawada, H., C. Nishiyama, A. Takagi, T. Tokura, N. Nakano, K. Maeda, N. Mayuzumi, S. Ikeda, K. Okumura, and H. Ogawa. 2005. Transcriptional regulation of ATP2C1 gene by Sp1 and YY1 and reduced function of its promoter in Hailey-Hailey disease keratinocytes. *J. Invest. Dermatol.* 124: 1206–1214.
31. Kumar, D., A. Ray, and B. K. Ray. 2009. Transcriptional synergy mediated by SAF-1 and AP-1: critical role of N-terminal polyalanine and two zinc finger domains of SAF-1. *J. Biol. Chem.* 284: 1853–1862.
32. Lahlil, R., E. Lécuyer, S. Herblot, and T. Hoang. 2004. SCL assembles a multifactorial complex that determines glycophorin A expression. *Mol. Cell. Biol.* 24: 1439–1452.
33. Lécuyer, E., S. Herblot, M. Saint-Denis, R. Martin, C. G. Begley, C. Porcher, S. H. Orkin, and T. Hoang. 2002. The SCL complex regulates c-kit expression in hematopoietic cells through functional interaction with Sp1. *Blood* 100: 2430–2440.
34. Walsh, J. C., R. P. DeKoter, H. J. Lee, E. D. Smith, D. W. Lancki, M. F. Gurish, D. S. Friend, R. L. Stevens, J. Anastasi, and H. Singh. 2002. Cooperative and antagonistic interplay between PU.1 and GATA-2 in the specification of myeloid cell fates. *Immunity* 17: 665–676.
35. Newton, A., J. Mackay, and M. Crossley. 2001. The N-terminal zinc finger of the erythroid transcription factor GATA-1 binds GATC motifs in DNA. *J. Biol. Chem.* 276: 35794–35801.
36. Hong, W., M. Nakazawa, Y. Y. Chen, R. Kori, C. R. Vakoc, C. Rakowski, and G. A. Blobel. 2005. FOG-1 recruits the NuRD repressor complex to mediate transcriptional repression by GATA-1. *EMBO J.* 24: 2367–2378.
37. Rodriguez, P., E. Bonte, J. Krijgsveld, K. E. Kolodziej, B. Guyot, A. J. Heck, P. Vyas, E. de Boer, F. Grosveld, and J. Strouboulis. 2005. GATA-1 forms distinct activating and repressive complexes in erythroid cells. *EMBO J.* 24: 2354–2366.
38. Hamlett, I., J. Draper, J. Strouboulis, F. Iborra, C. Porcher, and P. Vyas. 2008. Characterization of megakaryocyte GATA1-interacting proteins: the corepressor ETO2 and GATA1 interact to regulate terminal megakaryocyte maturation. *Blood* 112: 2738–2749.
39. Merika, M., and S. H. Orkin. 1995. Functional synergy and physical interactions of the erythroid transcription factor GATA-1 with the Krüppel family proteins Sp1 and EKLF. *Mol. Cell. Biol.* 15: 2437–2447.
40. Hong, S. J., H. J. Choi, S. Hong, Y. Huh, H. Chae, and K. S. Kim. 2008. Transcription factor GATA-3 regulates the transcriptional activity of dopamine beta-hydroxylase by interacting with Sp1 and AP4. *Neurochem. Res.* 33: 1821–1831.

Antimicrobial Peptides Human β-Defensins and Cathelicidin LL-37 Induce the Secretion of a Pruritogenic Cytokine IL-31 by Human Mast Cells

François Niyonsaba,* Hiroko Ushio,* Mutsuko Hara,* Hidenori Yokoi,† Mitsutoshi Tominaga,‡ Kenji Takamori,‡ Naoki Kajiwara,§ Hirohisa Saito,§ Isao Nagaoka,¶ Hideoki Ogawa,* and Ko Okumura*

In addition to their microbiocidal properties, human β-defensins (hBDs) and cathelicidin LL-37 stimulate a number of mammalian cell activities, including migration, proliferation, and cytokine/chemokine production. Because hBDs and LL-37 cause mast cells to release pruritogens such as histamine and PGs, we hypothesized that these peptides would stimulate the secretion of a novel pruritogenic mediator IL-31, predominantly produced by T cells. hBDs and LL-37 enhanced IL-31 gene expression and IL-31 protein production and release in the human mast cell line LAD2, as well as in peripheral blood-derived cultured mast cells, suggesting that mast cells are another source of IL-31. Moreover, the expression of IL-31 was elevated in psoriatic skin mast cells, and hBD-2–4 and LL-37, but not hBD-1, enhanced its expression in vivo in rat skin mast cells. hBDs and LL-37 also induced the release of other pruritogenic mediators, including IL-2, IL-4, IL-6, GM-CSF, nerve growth factor, PGE_2, and leukotriene C_4, and increased mRNA expression of substance P. hBD- and LL-37–mediated IL-31 production/release was markedly reduced by pertussis toxin and wortmannin, inhibitors of G-protein and PI3K, respectively. As evidenced by the inhibitory effects of MAPK-specific inhibitors, hBD-2–4 and LL-37 activated the phosphorylation of MAPKs p38, ERK, and JNK that were required for IL-31 production and release. The ability of hBDs and LL-37 to stimulate the production and release of IL-31 by human mast cells provides a novel mechanism by which skin-derived antimicrobial peptides/proteins may contribute to inflammatory reactions and suggests a central role of these peptides in the pathogenesis of skin disorders. ***The Journal of Immunology*****, 2010, 184: 3526–3534.**

The skin generates a number of antimicrobial peptides/proteins (AMPs) that provide a front-line component in innate immunity and inhibit microbial invasion; however, characterization of their activity as solely antimicrobial might be an oversimplification of the diverse functions of these molecules. In fact, there is a growing body of evidence suggesting that, apart from exhibiting a broad spectrum of microbiocidal properties, AMPs display additional activities that are related to stimulation and modulation of the cutaneous immune system. These diverse functions include chemoattraction and activation of immune and/or inflammatory cells, enhancement of the production of cytokines and chemokines, acceleration of angiogenesis, promotion of wound healing, neutralization of harmful microbial products, and bridging of both innate and adaptive immunity (1).

The major AMPs found in humans are defensins and cathelicidins. Human defensins are divided into α- and β-defensins based on gene organization, cellular location, expression pattern, and disulfide bond connectivity (1, 2). In contrast to α-defensins, which are distributed in neutrophils and intestinal Paneth cells (3, 4), human β-defensins (hBDs) are mainly generated by the epithelia of several organs, including skin (1, 5). To date, four hBDs (hBD-1, -2, -3, and -4) have been identified in human skin. The first, hBD-1, is constitutively expressed by various epithelial tissues, particularly in the terminal layers of skin, urogenital tissue, and respiratory tissue (6, 7). hBD-2 was initially identified in psoriatic lesions in human epidermis, and has been shown to be inducible in activated normal keratinocytes (8, 9). Expression of hBD-1 and hBD-2 can be detected in monocytes, macrophages, and monocyte-derived dendritic cells, indicating that these peptides are not exclusively epithelial cell-associated AMPs (10). Like hBD-2, hBD-3 was first isolated from lesional psoriatic scales (11); however, it is also abundant in nonepithelial tissues (11). The expression of hBD-4 has been identified at the mRNA level, but the isolation of natural hBD-4 peptide has not yet been reported (12). hBD-4 is constitutively expressed in testis and gastric antrum, and it is inducible in differentiated human primary keratinocytes (13) and respiratory epithelial cells (12). Both hBD-1 and hBD-2 are overexpressed in monocytes on exposure to bacteria, LPS, or IFN-γ (10, 14), whereas hBD-2–4 are highly detected in keratinocytes stimulated by bacteria, TNF-α, IL-1β, IL-17 (for hBD-2), or IL-22 (for hBD-2 and hBD-3) (13, 15–17). Among hBDs, only hBD-3 expression is regulated by growth factors such as insulin-like growth factor-1 and TGF-α in keratinocytes (18). In respiratory epithelial cells, hBD-4 mRNA expression is amplified by exposure to bacteria or to PMA (12).

*Atopy (Allergy) Research Center; †Department of Otorhinolaryngology, and ¶Department of Host Defense and Biochemical Research, Juntendo University School of Medicine; §Department of Allergy and Immunology, National Research Institute for Child Health and Development, Tokyo; and ‡Institute for Environment and Gender Specific Medicine, Juntendo University School of Medicine, Chiba, Japan

Received for publication March 5, 2009. Accepted for publication January 21, 2010.

This work was supported in part by a Grant-in-Aid for Scientific Research from the Ministry of Education, Culture, Sports, Science and Technology, Japan and by the Atopy (Allergy) Research Center, Juntendo University, Tokyo, Japan.

Address correspondence and reprint requests to François Niyonsaba, Juntendo University School of Medicine, 2-1-1 Hongo, Bunkyo-ku, Tokyo 113-8421, Japan. E-mail address: francois@juntendo.ac.jp

Abbreviations used in this paper: AMP, antimicrobial peptide/protein; Ctrl, control; EIA, enzyme immunoassay; hCAP18, human cationic antibacterial protein of 18 kDa; hBD, human β-defensin; FPRL1, formyl peptide receptor-like 1; LT, leukotriene; Med, medium; NGF, nerve growth factor; PTx, pertussis toxin; SCF, stem cell factor; Sub P, substance P; Sup, supernatant; Wort, wortmannin.

www.jimmunol.org/cgi/doi/10.4049/jimmunol.0900712

The name cathelicidin defines a diverse group of cationic peptides based on their evolutionarily highly conserved cathelin-like N-terminal domain and a structurally variable cationic AMP at the C terminus (19). The unique human cathelicidin is designated human cationic antibacterial protein of 18 kDa (hCAP18) because of its very close relationship to the CAP18 found in rabbits (20). Mature AMP derived from hCAP18 is termed LL-37; it begins with two leucine residues and has 37 aa residues. LL-37 is found in specific granules of neutrophils, but is also expressed in NK cells, γδT cells, B cells, and monocytes (21), mast cells (22), keratinocytes (23), and various epithelial cells (24, 25). 1,25-Dihydroxyvitamin D_3 is thought to be a potent inducer of hCAP18/LL-37 mRNA transcription, and it seems that the presence of vitamin D_3 is essential for cathelicidin induction in skin infection and wounds (26–28). In contrast to colon epithelium, LL-37 expression is enhanced in keratinocytes by insulin-like growth factor-1 and TGF-α (29). Similar to hBDs, the expression of LL-37 is augmented in various skin disorders (1); however, these AMPs are downregulated in atopic dermatitis (30). This explains why patients with atopic dermatitis often demonstrate increased susceptibility to bacterial and viral infections, particularly *Staphylococcus aureus*.

Apart from their direct antimicrobial functions, hBDs and LL-37 activate several types of cells, including neutrophils, keratinocytes, and monocytes (1). Furthermore, hBDs and LL-37 have been reported to chemoattract and degranulate murine, rat and human mast cells (31–35), subsequently increasing vascular permeability via mast cell activation (35, 36). Although the mechanism by which hBDs and LL-37 activate mammalian cells is not yet well understood, it has been shown that these peptides bind to functional receptors to stimulate various types of cells. For example, hBD-1–3 likely bind to the chemokine receptor CCR6 on dendritic cells, T cells, and monocytes (37, 38), and LL-37 reportedly activates formyl peptide receptor-like 1 (FPRL1) (39), purinergic receptor $P2X_7$ (40), and transactivates epidermal growth factor receptor (41). Moreover, hBDs and LL-37 are reported to trigger MAPK pathways during the secretion of cytokines and chemokines in various cell types (1).

Because hBDs and LL-37 cause mast cells to release histamine and PGD_2, both of which are known as pruritogenic mediators (42, 43), we speculated that hBDs and LL-37 might stimulate IL-31 expression and/or secretion. IL-31 is a newly discovered member of the gp130/IL-6 cytokine family, and it is produced mainly by activated $CD4^+$ T cells (44). Recently, IL-31 has been shown to be involved in the development of chronic dermatitis through the induction of severe pruritus in transgenic mice with lymphocyte-specific overexpression of IL-31 (44). Skin IL-31 mRNA levels are significantly higher in NC/Nga mice with scratching behavior (45), and this cytokine is overexpressed in pruritic atopic dermatitis but not in nonpruritic psoriatic lesions compared with human healthy skin (46). Moreover, acute allergic contact dermatitis, a skin disease featuring skin inflammation and pruritus, has also been associated with higher IL-31 mRNA levels than those seen in healthy skin (47). Together, these observations provide evidence for a pivotal role of IL-31 in the induction of pruritus in skin disorders.

In this study, we show that human mast cells constitute another source of IL-31, and that secretion of IL-31 from mast cells is increased upon stimulation with hBDs and LL-37. These peptides also induced the release of several pruritogenic mediators, including cytokines, nerve growth factor (NGF), PGE_2, and leukotriene (LT) C_4, from mast cells. We also demonstrate that hBDs and LL-37 activate MAPKs and that the secretion of IL-31 is controlled by G protein, PI3K, and MAPK pathways. Thus, hBDs and LL-37 may contribute to skin inflammatory responses by causing mast cells to secrete IL-31 and other pruritogenic factors.

Materials and Methods

Reagents

Antimicrobial peptides hBD-1, hBD-2, hBD-3 and hBD-4 were obtained from the Peptide Institute (Osaka, Japan). LL-37 (L^1LGDFFRKSKEKIGKEFKRIVQRIKDFLRNLVPRTES^{37}) was synthesized by the solid-phase method on a peptide synthesizer (model PSSM-8; Shimadzu, Kyoto, Japan) by fluoroenylmethoxycarbonyl chemistry, and the molecular mass was confirmed on a mass spectrometer (model TSQ 700; Thermo Quest Finnigan, Manchester, U.K.). Human myeloma IgE was obtained from Calbiochem (La Jolla, CA); mouse anti-human IgE and mouse anti-rat mast cell (clone AR32AA4, 1:100) Abs were from BD Pharmingen (San Diego, CA). Rabbit anti-rat IL-31 Ab (1:100) was purchased from Abcam (Cambridge, MA). Mouse anti-human IL-31 Ab (clone 308202, 1:50) was from R&D Systems (Minneapolis, MN), and mouse anti-human mast cell tryptase Ab (clone G3, 1:1500) was obtained from Chemicon (Temecula, CA). Secondary Abs conjugated with Alexa Fluor 488 or Alexa Fluor 594 were from Invitrogen (Carlsbad, CA). Rabbit polyclonal anti-phosphorylated p38, ERK and JNK Abs, and p38, ERK and JNK Abs were purchased from Cell Signaling Technology (Beverly, MA). The inhibitors SB203580 (Sigma-Aldrich, St. Louis, MO), PD98059 (Cell Signaling Technology) and SP600125 (Calbiochem) were used to study the MAPK pathways involved in the activation of mast cells. Pertussis toxin and wortmannin were obtained from Sigma-Aldrich.

Cell culture and stimulation

The LAD2 cell line isolated from the bone marrow of a patient with mast cell leukemia was a gift from Dr. Arnold Kirshenbaum (National Institutes of Health, National Institute of Allergy and Infectious Diseases, Bethesda, MD) (48). These cells were grown in Stem Pro-34 medium containing nutrient supplements (Invitrogen), supplemented with 2 mM L-glutamine (Invitrogen), 100 IU/ml penicillin and 100 μg/ml streptomycin (Meiji Seika, Tokyo, Japan), and 100 ng/ml human stem cell factor (SCF) (Wako, Osaka, Japan). Cell culture medium was hemidepleted every week with fresh medium. Human peripheral blood-derived cultured mast cells were obtained using previously described methods with some modifications (49). G-CSF-mobilized human peripheral bloods $CD34^+$ cells (Veritas Corporation, Tokyo, Japan) were cultured in serum-free Iscove's methylcellulose medium (Stem Cell Technologies, Vancouver, BC, Canada) containing 200 ng/ml SCF, 50 ng/ml IL-6 and 2.5 ng/ml IL-3 (PeproTech, London, U.K.), 100 IU/ml penicillin, and 100 μg/ml streptomycin (Life Technologies, Grand Island, NY). At 6 wk, the methylcellulose medium was dissolved in PBS, and the cells were then resuspended and cultured in IMDM supplemented with 100 ng/ml SCF, 50 ng/ml IL-6, 5% FCS, 55 μM 2-ME, 100 IU/ml penicillin, and 100 μg/ml streptomycin. Hemidepletions of media were performed weekly by adding fresh media. The final purity of mast cells always exceeded 95%. Following incubation with various doses of hBDs or LL-37, mast cells at a final concentration of $1–2 \times 10^6$ cells/ml were centrifuged; the supernatants were used for ELISA, and the pellets were used for total RNA extraction or Western blotting analysis.

ELISA

IL-2, IL-4, IL-6, IL-8, IL-31, GM-CSF, TNF-α, NGF, LTC_4, and PGE_2 released into cell-free supernatants from cultures of mast cells stimulated with hBD-1–4 or LL-37 or from nonstimulated control cultures were measured with ELISA or enzyme immunoassay (EIA). The ELISA kits specific for IL-2, IL-4, IL-6, IL-8, IL-31, GM-CSF, NGF, and TNF-α were purchased from R&D Systems, whereas EIA kits for LTC_4 and PGE_2 were obtained from Cayman Chemical Company (Ann Arbor, MI). Supernatants were stored at −20°C until used for ELISA or EIA, according to the manufacturer's instructions. In some experiments, mast cells were pretreated with different inhibitors for 2 h before stimulation with hBDs and LL-37.

Treatment of mast cells with pertussis toxin, wortmannin, and MAPK inhibitors

The effects of G-protein inhibitor pertussis toxin, PI3K inhibitor wortmannin, and MAPK specific inhibitors SB203580 (p38 inhibitor), PD98059 (ERK inhibitor), and SP600125 (JNK inhibitor) were investigated by incubating LAD2 mast cells with pertussis toxin (200 ng/ml), wortmannin (20 μM), SB203580 (10 μM), PD98059 (10 μM), or SP600125 (20 μM) for 2 h at 37°C in culture medium. Cells were then stimulated with hBDs or LL-37 for 12 h, and ELISA for IL-31 was performed as above.

Immunofluorescence staining

All animal procedures were approved by the institutional Animal Care and Use Committee of Juntendo University School of Medicine. Sprague-Dawley rats weighing 300–400 g were injected intradermally with 50 μl hBDs or LL-37 (500 ng) into one side of the ear and with vehicle (0.9% normal saline) into the other ear. After 12 h, rats were sacrificed, and small pieces of the ears were embedded in optical cutting temperature compound (Sakura Finetechnical, Tokyo, Japan) and frozen in liquid nitrogen. Cryosections (5 μm) were cut using a CM1850 cryostat (Leica, Wetzlar, Germany) and mounted on silane-coated glass slides. After blocking in PBS with 5% normal goat serum (Chemicon) and 2% BSA (Sigma-Aldrich), cryosections were double-labeled with anti-rat IL-31 and anti-rat mast cell Abs for 2 h at room temperature. After washing with PBS, the sections were incubated with secondary Abs for 1 h at room temperature.

Human skin donors provided written informed consent for participation in this study that was conducted with the approval of the medical ethical committee of the Juntendo University Urayasu Hospital. As described previously (50), 3-mm punch biopsies were taken from normal abdominal skins of three healthy volunteers and from lesional abdominal skins of three patients with clinical appearance of psoriasis. Cryosections (7 μm) from 4% paraformaldehyde-fixed skins were cut, fixed with ice-cold acetone, and then blocked in PBS with 5% normal donkey serum (Chemicon) and 2% BSA. The sections were double-stained with Abs against human IL-31 at 4°C overnight and human mast cell tryptase for 1 h at room temperature, and then the secondary Abs were added to the sections for 1 h at room temperature. Immunolabeling controls were performed by either omitting primary Abs in the procedure or replacing them with normal IgG. Sections were mounted in Vectashield mounting medium with DAPI (Vector Laboratories, Peterborough, U.K.), and viewed with a confocal laser-scanning microscope DMIRE2 (Leica).

Western blot analysis

LAD2 cells (2×10^6 cells/ml) were incubated with hBDs, LL-37, or IgE/anti-IgE for 5–60 min. Following stimulation, cell lysates were obtained by lysing cells in lysis buffer (50 mM Tris-HCl (pH 8), 150 mM NaCl, 0.02% NaN_3, 0.1% SDS, 1% NP 40) containing protease inhibitor mixture, phosphatase inhibitor mixture 1 and mixture 2 (Sigma-Aldrich) prepared according to the manufacturer's specifications. Equal amounts of total protein were subjected to 12.5% SDS-PAGE. After nonspecific binding sites were blocked, the blots were incubated with polyclonal Abs against phosphorylated or unphosphorylated p38, ERK, and JNK overnight. The membrane was developed with an ECL detection kit (Amersham Pharmacia Biotech, Piscataway, NJ). To quantify band intensity, densitometry using the software program Image Gauge (LAS-4000plus; Fujifilm, Tokyo, Japan) was performed to allow correction for protein loading.

Total RNA extraction and quantitative real-time PCR

Total RNA was extracted from mast cells using Trizol reagent (BRL; Life Technologies, Rockville, MD), according to the manufacturer's instructions. First-strand cDNA was synthesized from 3 μg total RNA with oligo$(dT)_{12\text{-}18}$ primers using Superscript II RNase H$^-$ reverse transcriptase (Life Technologies), as described previously (51). Real-time PCR was performed using the TaqMan Universal PCR Master Mix (Applied Biosystems, Branchburg, NJ). Amplification and detection of target mRNA were analyzed using a 7500 Real-Time PCR System (Applied Biosystems), according to the manufacturer's instructions. IL-31 and substance P primer/probe sets were obtained from Applied Biosystems Assays-on-Demand. To standardize mRNA concentrations, transcript levels of the housekeeping gene β-actin were determined in parallel for each sample, and relative IL-31 or substance P transcript levels were corrected by normalization based on β-actin transcript levels.

Statistical analysis

Statistical analysis was performed using Student *t* test or one-way ANOVA with multiple comparison test (Prism 4, GraphPad Software, San Diego, CA), and $p < 0.05$ was considered to be significant. The results are shown as the mean ± SD.

Results

Antimicrobial hBDs and LL-37 induce IL-31 gene expression in human mast cells

Antimicrobial hBDs and LL-37 have been reported to induce the release of inflammatory mediators such as histamine and PGD_2 that are known to contribute to pruritus (32, 35). We therefore asked whether hBDs and LL-37 could also stimulate the expression of the novel pruritus-promoting cytokine IL-31, which has been reported to be produced predominantly by T cells (44). Incubation of LAD2 cells with various concentrations of hBD-1–4 or LL-37 resulted in significant, dose-dependent increases in IL-31 mRNA expression as analyzed by quantitative real-time PCR (Fig. 1). The effect of hBD-3 was stronger than that of other AMPs, with concentrations of hBD-3 as low as 1 μg/ml inducing significant levels of IL-31 mRNA expression. In preliminary experiments, we observed that the expression of IL-31 mRNA reached a peak within 6 h after exposure to 20 μg/ml hBD-1, and that on exposure to 10 μg/ml hBD-2–4 or LL-37 it reached a peak within 3 h; in both cases, the IL-31 mRNA level then gradually decreased and returned to baseline by 12 h (data not shown). We also confirmed by trypan blue exclusion and measurement of lactate dehydrogenase activity that hBDs and LL-37 were not cytotoxic at the concentrations used in our study (data not shown).

hBDs and LL-37 stimulate IL-31 production/release by human mast cells

Because hBDs and LL-37 increased IL-31 mRNA levels in mast cells, we investigated whether they could also boost the production of IL-31 protein. After stimulation of LAD2 cells with 20 μg/ml hBD-1, 10 μg/ml hBD-2–4, or 10 μg/ml LL-37 for 3–24 h, the release of IL-31 protein in cell-free supernatants was determined using a specific ELISA kit. As shown in Fig. 2*A*, hBD-2–4 and LL-37 significantly induced the release of IL-31. Although 20 μg/ml hBD-1 markedly increased IL-31 mRNA expression, as seen in Fig. 1, the same concentration had no significant effect on IL-31 release. Doses of hBD-1 >20 μg/ml did not further enhance IL-31 release (data not shown). The augmentation of IL-31 release by mast cells after hBD and LL-37 activation raised the question of

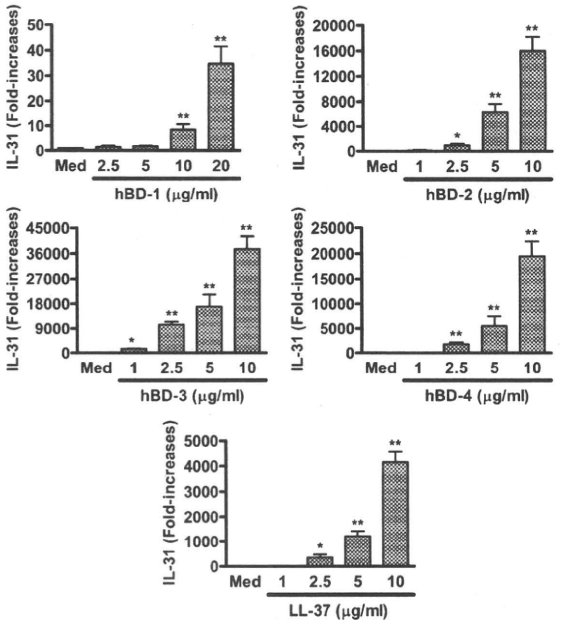

FIGURE 1. hBDs and LL-37 increase gene expression of IL-31 in LAD2 mast cells. LAD2 cells (2×10^6) were stimulated with the indicated concentrations (1–20 μg/ml) of hBD-1–4 or LL-37 for 6 h for hBD-1, and for 3 h for hBD-2–4 and LL-37. After incubation, total RNA was extracted and converted into cDNA, and real-time PCR was performed to analyze changes in IL-31 gene expression. Each bar shows the mean ± SD from four to six independent experiments, each of which was run in triplicate. Values represent fold increases in gene expression compared with cells incubated with medium alone. *$p < 0.01$; **$p < 0.001$. Med, medium.